E2F1 and E2F2 induction in response to DNA damage preserves genomic stability in neuronal cells

Daniela S. Castillo[1], Anna Campalans[2,3], Laura M. Belluscio[1], Abel L. Carcagno[1,4], J. Pablo Radicella[2,3], Eduardo T. Cánepa[1,*], Nicolás Pregi[1,*]

[1]Laboratorio de Biología Molecular, Departamento de Química Biológica, Facultad de Ciencias Exactas y Naturales, Universidad de Buenos Aires, Ciudad de Buenos Aires C1428EGA, Argentina

[2]CEA, Institute of Cellular and Molecular Radiobiology, Fontenay aux Roses F-96265, France

[3]UMR967 INSERM / Universités Paris Diderot et Paris Sud, Fontenay aux Roses F-92265, France

[4]Present address: Laboratorio de Genética del Desarrollo Neural, Fundación Instituto Leloir, Ciudad de Buenos Aires C1405BWE, Argentina

*Correspondence to: Nicolás Pregi; Email: npregi@qb.fcen.uba.ar; Eduardo T. Cánepa; Email: ecanepa@qb.fcen.uba.ar

Running title: E2F1 and E2F2 upregulation maintains genome integrity

Keywords: DNA damage response; DNA repair; E2F transcription factor; genomic stability; neuronal cells.

25 **Abbreviations**: ODN, oligodeoxynucleotide; NCS, neocarzinostatin; ASCAT, CAT
26 antisense; ASE2F1, E2F1 antisense; ASE2F2, E2F2 antisense; wt E2F DO, wild-type E2F
27 decoy oligodeoxynucleotide; mut E2F DO, mutant E2F decoy oligodeoxynucleotide.

ABSTRACT

E2F transcription factors regulate a wide range of biological processes, including the cellular response to DNA damage. In the present study, we examined whether E2F family members are transcriptionally induced following treatment with several genotoxic agents, and have a role on the cell DNA damage response. We show a novel mechanism, conserved amongst diverse species, in which *E2F1* and *E2F2*, the latter specifically in neuronal cells, are transcriptionally induced after DNA damage. This upregulation leads to increased E2F1 and E2F2 protein levels as a consequence of *de novo* protein synthesis. Ectopic expression of these E2Fs in neuronal cells reduces the level of DNA damage following genotoxic treatment, while ablation of E2F1 and E2F2 leads to the accumulation of DNA lesions and increased apoptotic response. Cell viability and DNA repair capability in response to DNA damage induction are also reduced by the E2F1 and E2F2 deficiencies. Finally, E2F1 and E2F2 accumulate at sites of oxidative and UV-induced DNA damage, and interact with γH2AX DNA repair factor. As previously reported for E2F1, E2F2 promotes Rad51 foci formation, interacts with GCN5 acetyltransferase and induces histone acetylation following genotoxic insult. The results presented here unveil a new mechanism involving E2F1 and E2F2 in the maintenance of genomic stability in response to DNA damage in neuronal cells.

INTRODUCTION

The E2F family of transcription factors is encoded by eight genes, *E2F1-E2F8*, which give rise to nine different proteins. The two E2F3 proteins –E2F3a and E2F3b– are the product of alternative use of promoters of the E2F3 locus. [1-2] Traditionally, E2F family members have been subdivided into two groups based on their transcriptional activities, structures and

53 interactions with the pocket proteins Retinoblastoma protein (pRB), Retinoblastoma-like
54 protein 1 (p107) and Retinoblastoma-like protein 2 (p130). E2F1, E2F2 and E2F3a, that only
55 bind pRB, constitute the 'activator' E2Fs due to their ability to activate transcription of E2F
56 target genes. E2F3b and E2F4-E2F8 are considered the 'repressor' E2Fs since they are
57 capable of repressing the expression of mostly overlapping sets of target genes. E2F3b, E2F4
58 and E2F5 exert their repressive function in association with a pRB family member, while
59 E2F6-E2F8 repress transcription in a pocket protein-independent manner as they lack the
60 pocket protein binding domain.[3-6]
61 Despite the fact that E2Fs were originally described to play a pivotal role in cell cycle
62 control,[7-8] it has become clear that they participate in the regulation of a plethora of biological
63 processes, including the cellular response to DNA damage. It was first reported that E2F1
64 protein levels increase upon treatment with several DNA damaging agents. [9-12] Further studies
65 revealed that E2F4 levels decrease whereas E2F3a, E2F7 and E2F8 are upregulated following
66 DNA damage.[13-15]
67 E2F1 is the best studied family member with respect to its regulation and function following
68 genotoxic stress. Its participation in the DNA damage response can be described from three
69 different angles.[16] First, E2F1 undergoes posttranslational modifications in response to DNA
70 damage. E2F1 is phosphorylated on serine 31 by ataxia-telangiectasia mutated (ATM) and
71 ataxia-telangiectasia and Rad3-related (ATR) kinases, [12] and on serine 364 by Checkpoint
72 kinase 2 (Chk2). [17] It is also acetylated on lysines 117, 120 and 125 by either p300/CREB-
73 binding protein (p300/CBP) or p300/CREB-binding protein-associated factor (P/CAF)
74 acetyltransferases.[18-19] These modifications contribute to E2F1 stabilization and explain the
75 elevated E2F1 protein levels observed after genotoxic insult.[12, 17-18] Second, E2F1
76 transactivation ability following DNA damage is regulated through its interaction with
77 specific protein partners. E2F1-pRB complexes repress transcription when they are

78 associated with nucleosome remodeling proteins, methyltransferases, or histone
79 deacetylases,[20-22] but activate it upon interaction with histone acetyltransferases. [23-24] Finally,
80 E2F1 is recruited to sites of DNA lesions and promotes the recruitment of repair factors,
81 suggesting a role for E2F1 in DNA repair.[25-27]
82 It was also shown that UV irradiation induces the transcription of *E2F1*, resulting in
83 increased E2F1 protein levels. [28] Therefore, two parallel mechanisms contribute to E2F1
84 induction in response to DNA damage: the posttranslational modifications and consequent
85 protein stabilization, and the enhanced transcription that leads to *de novo* protein synthesis.
86 Recent observations have also demonstrated that other E2F family members are
87 transcriptionally induced upon treatment with doxorubicin. [14] These findings suggest that
88 DNA damage itself, and not a signal generated by a particular genotoxic agent, is at the origin
89 of the upregulation of *E2F1* gene transcription. The aim of the present work is to examine
90 whether various E2F family members are transcriptionally induced following treatment with
91 several genotoxics in different species –with special interest on a neuronal cell based system–
92 and have a role on the cell DNA damage response.
93 Here, we show that *E2F1* and *E2F2*, the latter specifically in neuronal cells, are
94 transcriptionally induced upon DNA damage. This upregulation contributes to the
95 augmentation of E2F1 and E2F2 protein levels, which are active in their transcription
96 regulation functions. Importantly, ectopic expression of these E2Fs in neuronal cells reduces
97 the accumulation of DNA damage following treatment with genotoxic agents. Conversely,
98 ablation of E2F1 and E2F2 leads to increased levels of DNA damage and apoptotic response,
99 and also reduces cell viability and DNA repair capability upon genotoxic stress. Moreover,
100 we show that E2F1 and E2F2 accumulate at sites of oxidative and UV-induced DNA damage,
101 and associate with γH2AX DNA repair factor. Finally, as it was formerly established for
102 E2F1,[25, 27] we demonstrate that E2F2 promotes Rad51 foci formation, interacts with GCN5

103 acetyltransferase and induces histone acetylation following genotoxic insult. In summary, the
104 evidence presented here establishes a new mechanism involving E2F1 and E2F2 in the
105 response to DNA damage and the maintenance of genomic integrity in neuronal cells.
106
107 **RESULTS**
108
109 *E2F1 and E2F2 are induced upon DNA damage in neuronal cells*
110 In order to evaluate the response of *E2F* genes to DNA damage, we first performed a time
111 course study of the mRNA levels of *E2F1-5* after exposure of cells to several genotoxic
112 agents differing in their mechanism of action and the resulting lesions. The genotoxics used
113 were neocarzinostatin (NCS) –a radiomimetic drug that generates double strand breaks–,
114 hydrogen peroxide (H_2O_2) –known to produce oxidative stress and consequently single-strand
115 breaks (SSBs) and base damage– and UV-C (UV) irradiation –which causes essentially
116 pyrimidine dimers–. Northern blot assays on HepG2 cells revealed an increase of *E2F1*
117 mRNA levels upon treatment with each of the genotoxic agents used (Supplementary Fig.
118 1A). No such changes were detected for the other family members studied. *E2F1* mRNA
119 raise was also observed in HEK293 cells (Supplementary Fig. 1B). Next, we used the same
120 approach on neuronal cell lines and found that both *E2F1* and *E2F2* transcripts were
121 augmented after treatment with each of the DNA damaging agents in SH-SY5Y (Fig. 1A),
122 Neuro-2a, HN9 and PC12 cells (Supplementary Fig. 2A-C). Finally, *E2F1* and *E2F2*
123 transcript levels were increased in rat primary hippocampal neuron cultures irradiated with
124 UV (Supplementary Fig. 2D), strengthening the notion that the *E2F2* mRNA augmentation in
125 response to DNA damaging agents is characteristic of neuronal cells. Together, these results
126 indicate that in response to DNA damage there is an *E2F1* mRNA increase in all cell types,
127 while *E2F2* mRNA raise would be restricted to neuronal cells. As proposed, this response

128 appears to be independent of the type of DNA damage induced and shared by several species.
129 The specificity of the probes used in Northern blot assays is shown in Supplementary Fig. 3.
130 Next, to rule out the possibility that *E2F1* and *E2F2* mRNA increase observed after the
131 genotoxic stress was a consequence of transcript stabilization, we studied the effect of
132 blocking transcription through actinomycin D treatment. To examine this, cells were
133 incubated with actinomycin D for 3 h, exposed to genotoxic agents and harvested for a
134 Northern blot assay at the time the maximum mRNA levels had been observed.
135 Transcriptional inhibition prevented *E2F1* and *E2F2* mRNA accumulation induced by the
136 three types of DNA damage (Fig. 1B). These data suggest that the upregulation of *E2F1* and
137 *E2F2* mRNA by genotoxics is due to enhanced transcription.
138 In light of these findings, we examined whether the increases in *E2F1* and *E2F2* mRNA
139 levels resulted in an elevation of their protein levels. Western blot assays on SH-SY5Y cells
140 revealed an increase in E2F1 and E2F2 proteins upon exposure to each of the genotoxics
141 tested (Fig. 1C). Surprisingly, while the induction of E2F1 was expected due to its increased
142 transcription and the reported stabilization of the protein, [12, 17-18] the induction of E2F2 was
143 detected not only in neuronal cells, but also in HEK293 cells (Supplementary Fig. 4) where
144 we did not observe an increase in *E2F2* mRNA level in response to the DNA damaging
145 treatments (Supplementary Fig. 1B), suggesting a stabilization of the protein after the
146 genotoxic insult. To test this notion, we evaluated whether ectopically expressed E2F2 could
147 be stabilized by UV light. Western blot assays on SH-SY5Y cells transfected either with
148 E2F1-GFP or E2F2-GFP vectors and exposed to UV showed a significant increase in the
149 exogenously expressed E2F1 or E2F2 detected with anti-GFP tag antibody (Fig. 1D,E). Since
150 the expression of these E2Fs is driven by a promoter that does not respond to UV treatment
151 (Fig. 1F), these results suggest that E2F2 levels are increased by a posttranslational

152 mechanism in response to DNA damage, and confirm E2F1 stabilization by genotoxic stress
153 as previously reported.[12, 17-18]
154 Finally, to assess whether E2F1 and E2F2 increases upon genotoxic stress were a
155 consequence –at least partially– of *de novo* protein synthesis, we examined the effect of
156 inhibiting this process by treating cells with cycloheximide. Cells pre-incubated for 3 h with
157 cycloheximide were harvested and analyzed by Western blot assays 0, 60 and 90 minutes
158 after the times maximum proteins levels had been detected post-genotoxic treatment: 8 h for
159 E2F1 and 2 h for E2F2 (Fig. 1G). Results revealed that *de novo* protein synthesis inhibition
160 blocked E2F1 and E2F2 induction in response to UV irradiation (Fig. 1H). E2F1 increase in
161 mock-treated cells might be due to the unspecific stabilization by cycloheximide of some
162 mRNAs.[29] Therefore, these results indicate that E2F1 and E2F2 are *de novo* synthesized
163 following DNA damage.
164
165 *E2F1 and E2F2 induced by DNA damage are transcriptionally active*
166 To address whether the induced E2F1 and E2F2 are active in their transcription regulation
167 functions, we initially transfected neuronal cells with pE2F-CAT or pΔE2F-CAT reporter
168 plasmids and treated them with the DNA damaging agents. pE2F-CAT encodes the
169 chloramphenicol acetyltransferase (CAT) reporter gene driven by adenovirus E2 core
170 promoter and four copies of the E2F DNA binding sequence, while pΔE2F-CAT lacks
171 them.[30] When compared to mock-treated control cells, we observed an increase in pE2F-CAT
172 activity in cells exposed to DNA damage (Fig. 2A). Consequently, we sought to distinguish
173 between the contributions to this increased transactivation capability of the *de novo*
174 synthesized E2F1 and E2F2 from that of the stabilized E2F after genotoxic treatment. To this
175 purpose cells were transfected with pE2F-CAT along with E2F1 or E2F2 antisense
176 oligodeoxynucleotides (ODNs) –ASE2F1 and ASE2F2 respectively– (Supplementary Fig. 5),

177 which were designed to block protein synthesis, or with wild-type E2F decoy ODN (wt E2F
178 DO) containing E2F consensus sequences that would sequester cellular E2F away from its
179 target gene promoters, [31] hence abolishing both contributions. After subjecting these cells to
180 DNA damaging agents, we observed that transfection with ASE2F1 or ASE2F2 led to an
181 impaired CAT induction in response to the three genotoxic agents tested (Fig. 2B).
182 Interestingly, a more pronounced diminution on the reporter activity was detected with wt
183 E2F DO (Fig. 2C). Taken together, these data indicate that both transcription followed by *de*
184 *novo* protein synthesis and protein stabilization contribute to the pools of transcriptionally
185 active E2F1 and E2F2.
186
187 *E2F1 and E2F2 transcriptional induction in response to genotoxic stress requires ATM/ATR*
188 *and MEK kinases*
189 The cellular response to genomic instability implies the activation of a network of
190 transduction pathways. To investigate which pathways are involved in *E2F1* and *E2F2*
191 mRNA induction after genotoxic treatment, SH-SY5Y cells were incubated with specific
192 inhibitors before exposure to the DNA damaging agents and harvested 4 h later, which was
193 the time the maximum induction had been detected (Fig. 1A). Inhibition of both ATM and
194 ATR kinases, ATM kinase alone or MEK kinase –with caffeine, KU-55933 or PD-98059
195 respectively– abrogated *E2F1* and *E2F2* mRNA increase after genotoxic stress (Fig. 3).
196 Inhibition of PI3K or JNK kinases with LY-294002 or SP-600125 didn't have an effect on
197 *E2F1* and *E2F2* transcriptional induction in response to DNA damage. Similar results were
198 obtained with Neuro-2A and HN9 cells (Supplementary Fig. 6). Therefore, these results
199 imply that ATM/ATR and MEK kinases activities are required for the *E2F1* and *E2F2*
200 transcriptional upregulation following DNA damage.
201

202 *E2F1 and E2F2 induction prevents increased cellular DNA damage upon genotoxic stress*

203 In view of these findings, we addressed the possibility that E2F1 and E2F2 may play a
204 functional role in the neuronal cell response to genotoxic stress. Phosphorylation of histone
205 H2AX on serine 139 (γH2AX) is a well-known indicator of genomic injury. [32] We first
206 analyzed the levels of DNA damage by measuring the intensity of γH2AX in cells that
207 overexpressed E2F1 or E2F2. To do this, cells were transfected either with E2F1-GFP, E2F2-
208 GFP or GFP empty vector, fixed 30 minutes after UV irradiation and immunostained with
209 anti-γH2AX antibody (Fig. 4A). For the data analysis, cells were classified according to the
210 E2F fluorescence intensity observed –no E2F, low E2F or high E2F–, which reflects the
211 protein's expression level. Significantly lower γH2AX intensity levels were observed in
212 irradiated cells when E2F1 or E2F2 were upregulated (Fig. 4B). Besides, it is interesting to
213 note the inverse correlation between E2F1 expression and γH2AX staining. No reduction on
214 γH2AX intensity levels was detected by different expression levels of the GFP empty vector
215 –no GFP, low GFP or high GFP– (Fig. 4C), indicating that the observed decrease is indeed a
216 consequence of E2F1 and E2F2 upregulation. Finally, overexpression was confirmed by
217 E2F1 and E2F2 immunoblot of the endogenous and exogenously expressed proteins. There
218 was a 8.4-fold and 6.7-fold increase in E2F1 and E2F2 exogenous proteins respectively
219 compared to the endogenous proteins in basal conditions. These increases were higher than
220 the levels observed for the endogenous proteins at the time post-UV cells were fixed (30
221 minutes) and also at the time maximum protein levels had been previously observed post-UV
222 irradiation: 8 h for E2F1 and 2 h for E2F2 (Fig. 4D). Thus, these results suggest a role for
223 E2F1 and E2F2 in protecting neuronal cells against the accumulation of DNA damage in cells
224 exposed to UV.

225 Next, we decided to discriminate between the *de novo* protein synthesis from the stabilization
226 contributions to this E2F protection capability against DNA damage. To assess this, cells

227 were transfected with ASE2F1, ASE2F2 or wt E2F DO, exposed to genotoxics and analyzed
228 for γH2AX immunostaining (Fig. 5A; Supplementary Fig. 7). Either at 4 h or 10 h post-
229 genotoxic stress we observed an increased percentage of damaged cells in the presence of
230 ASE2F1 or ASE2F2 (Fig. 5B,C), as well as with wt E2F DO (Fig. 5D,E). It is worth noting
231 that the temporal analysis using the antisense ODNs revealed that *E2F1* and *E2F2*
232 transcriptional induction plays a role in regulating the level of DNA damage in neuronal cells
233 after genotoxic insult at different time points: E2F2 at an early and E2F1 at a later phase after
234 DNA damage. Moreover, our data suggests that *de novo* protein synthesis is the major
235 contribution in this regulation. To summarize, these results demonstrate that the E2F1 and
236 E2F2 increase upon genotoxic treatment, either from *de novo* protein synthesis or protein
237 stabilization, reduces the accumulation of DNA damage.
238 Finally, to assess whether E2F1 and E2F2 affect DNA repair capability in global genomic
239 repair, we measured the levels of UV induced-cyclobutane pyrimidine dimers (CPDs) in total
240 DNA extracted from neuronal cells that have been transfected with ASE2F1 or ASE2F2 and
241 exposed to UV light. Downregulation of E2F1 and E2F2 led to a delayed removal rate of
242 CPDs (Fig. 5F). While removal of CPD lesions started at 24 h post-UV irradiation and were
243 almost completely repaired at 48 h post-UV in control cells (ASCAT), significant amounts of
244 CPD lesions were still detected at this time point in E2F1 and E2F2 downregulated cells
245 (ASE2F1 and ASE2F2). Therefore, these results show that E2F1 and E2F2 enhance the
246 efficient removal of UV-induced CPD lesions.
247
248 *E2F1 and E2F2 upregulation reduces apoptotic response after genotoxic injury*
249 Cell death triggered by apoptosis is a common consequence of the excessive accumulation of
250 DNA damage. We therefore investigated whether E2F1 and E2F2 downregulation affected
251 the apoptotic response after genotoxic insult. To this purpose, we first measured caspase-3

252 activity in neuronal cells exposed to each of the three genotoxics. The results revealed that all
253 treatments led to an increase in caspase-3 activity (Supplementary Fig. 8). Next, we
254 transfected cells with ASE2F1, ASE2F2 or wt E2F DO and treated them with H_2O_2, the
255 genotoxic agent that triggered the maximum caspase-3 activity. Higher caspase-3 activity
256 levels were observed in the presence of ASE2F1 and ASE2F2 or wt E2F DO after H_2O_2
257 exposure (Fig. 6A,B). To confirm these findings, we also analyzed caspase-3 cleavage
258 through a Western blot assay in cells transfected with the ODNs and exposed to H_2O_2. Cells
259 treated with ASE2F1, ASE2F2 or wt E2F DO had increased levels of cleaved caspase-3 (Fig.
260 6C), suggesting that impairment of E2F1 and E2F2 induction after genotoxic treatment
261 triggers caspase-3 activation. Taken together, these findings point out a role for E2F1 and
262 E2F2 in protecting neuronal cells from apoptosis induced by DNA damage.
263
264 *E2F1 and E2F2 confer increased cellular resistance to DNA damaging agents*
265 We next investigated a potential physiological function of E2F1 and E2F2 in neuronal cell
266 response to genotoxic stress. Our findings implicating E2F1 and E2F2 in the reduction of the
267 apoptotic response and in the protection of neuronal cells from DNA damage after genotoxic
268 stress, raise the hypothesis that impairment of E2F1 and E2F2 induction might also affect cell
269 viability in response to DNA damage. To test this, we measured cell survival by MTT
270 reduction assay at different times during the 7 days following UV irradiation on cells that
271 have been previously transfected with ASE2F1, ASE2F2 or wt E2F DO. A significant
272 sensitization of cells transfected with ASE2F2 was observed, but not of those transfected with
273 ASE2F1 (Fig. 7A). Cells transfected with wt E2F DO also showed a reduced percentage of
274 viable cells (Fig. 7B).
275 To further analyze E2F1 and E2F2's long-term effects and biological relevance on cell
276 viability, we performed a clonogenic assay. Neuronal cells were transfected with ASE2F1,

277 ASE2F2 or wt E2F DO and treated with each of the three genotoxics (Fig. 7C). Ten days
278 later, we observed a reduced colony formation capability in cells transfected with ASE2F1 or
279 ASE2F2, and also in cells treated with wt E2F DO (Fig. 7D,E). In summary, the experiments
280 described above unveil a role for E2F2, and to a minor extent for E2F1, in cellular resistance
281 to different genotoxic stresses.
282
283 *E2F1 and E2F2 accumulate at sites of DNA lesion*
284 To investigate the mechanism of action of E2F1 and E2F2 following DNA damage, we
285 examined whether these proteins localize to the sites of DNA injury in neuronal cells. As a
286 first approach, we analyzed whether E2F1 and E2F2 were recruited to chromatin upon
287 genotoxic stress. To do this, we subjected cells to subcellular fractionation following
288 genotoxic insult, and collected the cytoplasmic and chromatin fractions which were analyzed
289 by electrophoresis. Immunoblots against E2F1 and E2F2 revealed an increase in E2F1 and
290 E2F2 proteins in the chromatin insoluble fraction after treatment with each of the genotoxic
291 agents, which peaks at 30 minutes post-DNA damage (Fig. 8A). Besides, quantification of
292 the cytoplasm and chromatin-associated E2F relative percentages shows an enrichment of
293 E2F1 and E2F2 in the chromatin fraction versus the cytoplasmic fraction following genotoxic
294 injury.
295 To address the possibility that E2F2 –as well as E2F1– accumulates at sites of DNA lesion,
296 we performed microirradiation experiments with a 405 nm laser coupled with the
297 photosensitizer Ro 19-8022 that promotes local formation of oxidative DNA damage, [33] in
298 neuronal cells previously transfected with E2F1-GFP or E2F2-GFP. We observed recruitment
299 of E2F1 and E2F2 to sites of DNA damage, but only in the presence of the photosensitizer
300 (Fig. 8B-E; Supplementary Movie S1,S2). These results suggest that both proteins localize to
301 the sites of induced oxidized bases but not in the SSBs generated by the 405 nm laser. [34]

302 Hence, in order to determine if E2F1 and E2F2 are recruited to sites of UV-induced lesions,
303 we carried out a modified chromatin immunoprecipitation assay on cells transfected with
304 E2F1-HA or E2F2-HA, after exposure to UV light. E2F1 and E2F2 were capable of pulling
305 down DNA fragments that contained the CPD DNA photoproduct, characteristic of UV-
306 induced DNA damage (Fig. 8F). JNK was used as a negative control of precipitation. Taken
307 together, these results indicate that E2F1 and E2F2 accumulate at sites of oxidative and UV-
308 induced DNA damage.
309 Finally, to study whether E2F1 and E2F2 interact with factors of the DNA repair machinery
310 such as γH2AX, we performed co-immunoprecipitation assays. Whole-cell extracts from
311 neuronal cells harvested 1 h post-NCS treatment were immunoprecipitated with anti-E2F1 or
312 anti-E2F2 antibodies and analyzed by immunoblot against γH2AX. Results showed that
313 γH2AX co-immunoprecipitates with endogenous E2F1 and E2F2 (Fig. 8G). E2F4 family
314 member was used as a negative control of co-immunoprecipitation since it didn't associate
315 with γH2AX in response to NCS-induced DNA damage. These results indicate an E2F1-
316 γH2AX and E2F2-γH2AX interaction following genotoxic injury.
317
318 *E2F2 promotes Rad51 foci formation and induces histone acetylation following DNA damage*
319 E2F1's role at sites of DNA lesion has been described in previous work, but E2F2's
320 nontranscriptional function is still unknown. It has been established that E2F1 promotes the
321 recruitment of DNA repair factors, such as Rad51, to sites of DNA double-strand breaks. [25]
322 Rad51 is the central recombinase in homologous recombination pathways. [35] To determine if
323 E2F2 is also involved in Rad51 recruitment to sites of DNA lesion, we performed
324 immunofluorescence assays in neuronal cells transfected with ASE2F2, fixed 1 h post-NCS
325 treatment and analyzed for Rad51 immunostaining (Fig. 9A). Downregulation of E2F2
326 impaired Rad51 foci formation in response to NCS-induced DNA damage (Fig. 9B). To

327 further confirm this result, Rad51 redistribution to sites of DNA damage was detected by
328 biochemical fractionation with Triton X-100. [36] Neuronal cells with ASE2F2 harvested 1 h
329 post-NCS treatment were fractionated into Triton soluble fraction, containing soluble
330 cytoplasmic proteins, or Triton insoluble fraction that contained chromatin-bound proteins.
331 Equal amounts of proteins from each fraction were analyzed by immunoblot against Rad51.
332 Results revealed a decrease in Rad51 recruitment to chromatin in the Triton insoluble fraction
333 in DNA-damaged cells transfected with ASE2F2 (Fig. 9C). Taken together, these results
334 indicate that E2F2, as it was reported for E2F1, is also implicated in genomic stability
335 maintenance through the recruitment of DNA repair factors to DNA double-strand breaks.
336 Previous work has demonstrated that E2F1 interacts with GCN5 acetyltransferase, promoting
337 its recruitment to sites of DNA damage, and that both E2F1 and GCN5 are necessary to
338 induce H3K9 acetylation in response to UV irradiation.[27] To evaluate if E2F2 is involved in a
339 similar epigenetic mechanism, we first performed co-immunoprecipitation assays to
340 determine if E2F2 also interacts with GCN5 following UV-induced DNA damage. Results
341 showed an association between E2F2 and GCN5 upon UV exposure (Fig. 9D). GCN5 has
342 been implicated in the acetylation of both H3 and H4 histones after UV irradiation. [37] To
343 assess whether loss of E2F2 affected global H4 acetylation in response to UV-induced DNA
344 damage, we analyzed acetylated H4 protein levels by Western blot in neuronal cells
345 downregulated for E2F2 and harvested 2 or 30 minutes following UV light exposure. We
346 observed that H4 acetylation induction in response to UV irradiation is impaired in E2F2
347 downregulated cells (Fig. 9E). Therefore, these results suggest that E2F2, like E2F1, is
348 involved in an epigenetic mechanism that promotes histone acetylation upon DNA damage,
349 which in turn would facilitate repair by increasing DNA repair machinery accessibility to
350 sites of damage.
351

352 **DISCUSSION**

353

354 In this work we report that *E2F1* and *E2F2*, the latter specifically in neuronal cells, are
355 transcriptionally induced in response to DNA damage. This novel mechanism, which is
356 common to the response to various genotoxic stresses and is conserved in several species,
357 contributes to increase E2F1 and E2F2 protein levels. Therefore, there are two parallel
358 mechanisms that lead to the upregulation of E2F1 and E2F2 following DNA damage: the
359 posttranslational modifications of the already synthesized E2F and consequent protein
360 stabilization and, on the other hand, the transcriptional *E2F* gene induction and *de novo*
361 protein synthesis. The resulting E2F1 and E2F2 act to promote DNA repair, leading to a
362 reduced apoptotic response and an increased cell survival capability, thereby conferring
363 resistance to genotoxic insult and cooperating in the maintenance of the genome integrity. It
364 should be emphasized that we show for the first time that E2F2 is upregulated following
365 genotoxic stress and plays a critical role in the DNA damage response.
366 E2F1 response to DNA damage has been subject of interest for many years. It has been well
367 established that E2F1 undergoes posttranslational modifications –such as phosphorylation
368 and acetylation– resulting in protein stabilization. [12, 17-18] Here, we show evidence that
369 suggests that E2F2 is also stabilized by a posttranslational mechanism in response to
370 genotoxic stress. Further studies to determine the types of modifications and enzymes
371 responsible for these modifications are required.
372 Our findings highlight a transcriptional mechanism for *E2F1* and *E2F2* induction upon DNA
373 damage, which depends on ATM/ATR and MEK kinases activities. A recent study has
374 reported an increase of the mRNAs of the three activating E2Fs –*E2F1*, *E2F2* and *E2F3a*– in
375 Saos2 cells upon overnight doxorubicin treatment. [14] We were unable to detect any *E2F3a*
376 induction with the cell lines and genotoxic insults used. Besides, we only observed *E2F2*

377 mRNA upregulation in neuronal cells. We don't know the reason for the discrepancy between
378 the results, although we can speculate differences are due to the cell type analyzed and the
379 dose of the DNA damaging agent used. Anyway, since we performed a broad study on the
380 time course changes of the mRNA levels of *E2F1-5* in a variety of cells (diverse tissues and
381 species) after exposure to several genotoxic agents, we propose that in response to DNA
382 damage there is a general mechanism resulting in *E2F1* and *E2F2* transcriptional induction,
383 the latter being restricted to neuronal cells. We presume that *E2F2* neuronal specifity
384 upregulation might rely on EGR-1 activity. EGR-1 transcription factor, which is expressed in
385 the nervous system, suits as a potential candidate since it has been shown to be upregulated –
386 mRNA and protein– in response to DNA damage, and to behave as a prosurvival factor
387 following ionizing and UV radiation. [38-42] Considering these evidence, we suggest EGR-1 as
388 an upstream regulator of E2F1 and E2F2 induction upon DNA damage. Although EGR-1 has
389 many potential binding sites in both E2F1 and E2F2 promoters, we speculate that in E2F2
390 promoter in neuronal cells it might associate with coactivators necessary to promote its'
391 transcription upon genotoxic stress. Additional studies are required to evaluate this
392 hypothesis and elucidate the mechanism underlying the basis of neuronal specificity of *E2F2*
393 transcriptional induction in response to DNA damage.
394 E2Fs transcriptional functions depend on the signals elicited by a particular type of DNA
395 damaging agent.[43-44] Many lines of evidence have indicated that the E2F1 protein increase in
396 response to genotoxic insult is associated to DNA damage-induced apoptosis. [12, 17, 43, 45]
397 Although it was always believed that the induction of apoptosis is a unique function of E2F1,
398 it was demonstrated that E2F2 and E2F3a can also activate pro-apoptotic genes. [46-47] In
399 contrast, here we show that the induced E2F1 and E2F2 reduce the apoptotic response
400 following DNA damage. This is consistent with the dual role these E2Fs may play upon
401 genotoxic stress, either promoting apoptosis or cell survival, and reinforces the notion that

402 this depends on the cell type and the source and dose of DNA damage. [48] In line with our
403 study, previous work has indicated a prosurvival role for E2F1. Transgenic E2F1 -/- mice
404 show enhanced levels of keratinocyte apotosis following UV-B radiation, whereas basal layer
405 keratinocyte specific overexpression of E2F1 suppresses UV-B-induced apoptosis. Besides,
406 inhibition of apoptosis induced by UV-B is correlated with increased efficiency on removal
407 of DNA photoproducts. [49-50] In addition, experiments have shown that in response to DNA
408 damage and ATM phosphorylation, E2F1 apoptotic activities are inhibited by binding to
409 TopBP1, and that this interaction results in E2F1 relocalization to BRCA1-containing repair
410 complexes.[51] E2F1 also participates in the recruitment of the Mre11 recombination/repair
411 complex to replication forks. [52] Furthermore, E2F1 regulates the transcription of the base
412 excision repair gene XRCC1 and thus contributes to DNA repair. [53] Collectively, these
413 findings point out a role for E2F1 in DNA damage checkpoints and/or repair. Consistently,
414 our results provide evidence that E2F1 and E2F2 upregulation upon genotoxic insult protects
415 neuronal cells from the accumulation of DNA damage. We can speculate that the observed
416 reduction in the apoptotic response following genotoxic stress is a consequence of an
417 increased DNA repair efficiency.
418 Interestingly, we show that E2F1 and E2F2 upregulation contributes to the maintenance of
419 the genome stability. Activator E2Fs can behave both as oncogenes and tumor suppressors
420 depending on the cellular context. [54-56] The oncogene activity is probably due to their ability
421 to promote cell proliferation, while the tumor suppression is believed to be a consequence of
422 their pro-apoptotic functions. The fact that we observed that E2F1 and E2F2 reduce
423 apoptosis, localize to the sites of DNA lesions and stimulate DNA repair in response to
424 genotoxic stress, is in agreement with earlier evidence that supports that E2F1 tumor
425 suppressor activity is in some cases unrelated to its apoptotic regulation but rather an
426 outcome of its nontranscriptional functions that facilitate DNA repair. E2F1 is localized to

427 sites of DNA double-strand breaks and UV-induced DNA damage, and promotes the
428 recruitment of DNA repair factors and chromatin modifying enzymes. [25, 27, 51] Our results add
429 a new component to this puzzle, E2F2, which as E2F1, is recruited to sites of oxidative and
430 UV-induced DNA damage, interacts with γH2AX DNA repair factor and GCN5
431 acetyltransferase, induces histone acetylation and promotes Rad51 foci formation. We also
432 demonstrate that upregulation of E2F1 and E2F2 protects against the accumulation of DNA
433 damage in cells exposed to UV light, whereas downregulation of either E2F1 or E2F2 leads
434 to increased levels of γH2AX following NCS, H_2O_2 or UV exposure, and impairs the removal
435 of CPD lesions after UV treatment. Therefore, these results suggest two possible roles for
436 E2F1 and E2F2 in DNA damage repair. First, a nontranscriptional function in which these
437 E2Fs localize to sites of DNA lesion upon genotoxic stress, and promote the recruitment of
438 DNA repair factors and chromatin modifying enzymes. Second, a transcriptional role
439 involving the expression of prosurvival genes in response to DNA damage. Given that we
440 show that the induced E2F1 and E2F2 are transcriptionally active, further experiments
441 designed to determine which are the E2F1 and E2F2 target genes that promote cell survival
442 following genotoxic insult are required.
443 DNA damage is a causal factor in neurodegenerative syndromes such as Alzheimer's and
444 Parkinson's diseases, with patients having an impaired DNA repair ability in their neural
445 tissues.[57] E2F1 and E2F2 represent potential targets for therapies to ameliorate the
446 neurological symptoms of these diseases. Thereby, a deeper understanding of the fine
447 molecular mechanisms that regulate these transcription factors' participation in the DNA
448 damage cellular response is needed.
449
450 **MATERIALS AND METHODS**
451

452 *Cell culture, genotoxic agents and transfections*

453 Neuro-2a murine neuroblastoma, HN9 murine hippocampal, HepG2 human hepatoma, and
454 HEK293 human embryonic kidney cells were grown in DMEM (Life Technologies)
455 supplemented with 10% fetal bovine serum (FBS), 100 U/ml penicillin, 100 μg/ml
456 streptomycin, 2 mM glutamine and 1 mM sodium pyruvate at 37°C in a 5% CO_2 humidified
457 atmosphere. The human neuroblastoma SH-SY5Y and rat pheochromocytoma PC12 cells
458 were maintained in DMEM (45%) and HAM F-12 (45%) (Life Technologies) at 37°C in 5%
459 CO_2 supplemented as indicated above. Rat primary hippocampal neuron cultures were
460 obtained from Wistar embryos of 18-19 gestation days as previously described, [58] and were
461 grown in Neurobasal medium (GIBCO) containing N2 supplement, B27 supplement, 100
462 U/ml penicillin, 100 μg/ml streptomycin, 2 mM glutamine and 1 mM sodium pyruvate at
463 37°C in 5% CO_2.

464 When indicated, cells were treated with 1 μM actinomycin D (Sigma-Aldrich), 10 μM
465 cycloheximide (Sigma-Aldrich), 50 ng/ml neocarzinostatin (Sigma-Aldrich), 100 μM
466 hydrogen peroxide, or were irradiated in open dishes with UV-C (UV) 40 J/m^2, 254 nm
467 (range 240-280 nm) at room temperature from a Philips ultraviolet lamp (TUV15WG15T8)
468 calibrated to deliver 2.5 J/m^2 sec. After UV exposure the medium was replaced and cells
469 were maintained at 37°C in 5% CO_2.

470 Cells were transfected either with polyethylenimine (PEI, Polysciences) or Lipofectamine
471 2000 reagent (Life Technologies), according to the manufacturer's instructions.

472

473 *Oligodeoxynucleotides and plasmids*

474 Single-strand oligodeoxynucleotides (ODNs) were synthesized with phosphodiester linkage
475 by Bio-Synthesis (Lewisville, TX). Antisense ODN sequences are: ASE2F1: 5'-
476 CCCGAGCAGGGCCTCCAGCGC-3' and ASE2F2: 5'-TCTGTGGGGCTCATCGCG-3'.

477 ASCAT: 5´-TGAAACTCACCCAGGGATTG-3´ and ASLUC: 5´-GCATACGACGAT
478 TCTGTGATTTG-3´ were used as internal controls. Circular dumbbell double-stranded
479 decoy ODN [31] wild-type E2F decoy: 5'-
480 ATGCGCGAAACGCGTTTTCGCGTTTCGCGCATAGTTTTCT-3' and mutant E2F decoy:
481 5'-ATCTAAACGCGTTTTCGCGTTTAGATTATAGTTTTCT-3' were annealed and ligated
482 for 24 h at 16°C with 1 unit of T4 DNA ligase (Life Technologies). The underlined sequences
483 correspond to the E2F consensus binding sites. In all cases, cells were transfected at a final
484 concentration of 1 μM ODN.
485 pE2F-CAT and pΔE2F-CAT plasmids were kindly provided by M. Imperiale. [59] The human
486 E2F1 expression plasmid E2F1-GFP was generously supplied by D. Johnson. [26] To obtain
487 E2F2-GFP fusion protein, the open reading frame of human E2F2 was inserted into a
488 pEGFP-C1 vector (Clontech) at the BglII/XbaI sites. E2F1-HA and E2F2-HA plasmids were
489 a gift from M. Campanero.[60]
490
491 *RNA extraction and Northern blotting analysis*
492 Total cellular RNA was isolated from cultures as described previously.[61] Briefly, for
493 Northern blotting analysis, 10 μg of total RNA were denatured, electrophoresed in 1%
494 glyoxal-agarose gels, and transferred to nylon membranes (Hybond N $^{+}$, GE Healthcare).
495 Membranes were sequentially hybridized with the indicated [^{32}P]-labelled probes and
496 radioactivity was detected using a PhosphorImager (FujiFilm BAS-1800II). Densitometric
497 analysis was performed using the NIH ImageJ software.
498
499 *Western blotting analysis*
500 Cells were lysed with RIPA buffer (50 mM Tris-HCl pH 7, 150 mM NaCl, 1% Triton X-100,
501 0.25% sodium deoxycholate, 1 mM EDTA pH 8 and 1X protease inhibitor cocktail

502 (Calbiochem)) and equal amounts of protein were resolved on SDS-PAGE. After transfer to a
503 nitrocellulose membrane (Hybond-ECL, GE Healthcare), analysis by immunoblotting was
504 performed using 1:100 E2F1 (sc-251), 1:100 E2F2 (sc-9967), 1:1000 cleaved caspase-3 (Cell
505 Signaling 9664), 1:3000 β-actin (sc-47778), 1:1000 GAPDH (sc-32233), 1:1000 Histone H3
506 (sc-8654-R), 1:1000 phospho-Histone H2A.X Ser139 (Upstate 05-636), 1:200 E2F4 (sc-866),
507 1:1000 Rad51 (sc-8349), 1:1000 GCN5 (sc-20698) and 1:2000 affinity purified polyclonal
508 anti-GFP antibodies. Secondary antibodies were from Sigma-Aldrich. The signal was
509 visualized with enhanced chemiluminiscence reagent (GE Healthcare) and LAS-1000 Image
510 Analyzer (Fujifilm). Densitometric analysis was performed using the NIH ImageJ software.
511
512 *Chloramphenicol acetyltransferase assay*
513 Neuro-2a cells were transfected with pE2F-CAT or pΔE2F-CAT along with pCEFL-β-
514 galactosidase for chloramphenicol acetyltransferase (CAT) assay. After 18 h, cells were
515 exposed to the genotoxic agents and harvested 24 h later. CAT activity was determined as
516 previously described[62] and normalized to β-galactosidase activity.
517
518 *Immunofluorescence*
519 SH-SY5Y or Neuro-2a cells were seeded onto glass coverslips and allowed to attach 24 h
520 before transfection with the specified plasmid or ODN. Genotoxic treatment was performed
521 18 h later and cells were fixed and immunostained as described, [63] using 1:500 anti-phospho-
522 Histone H2A.X Ser139 (Upstate 05-636) and 1:2000 Alexa Fluor 555 anti-mouse (Life
523 Technologies) antibodies, or 1:1000 anti-Rad51 (Calbiochem PC130) and 1:2000 Alexa
524 Fluor 488 anti-rabbit (Life Technologies) antibodies, and 1 μg/μl DAPI to visualize nuclei.
525 SH-SY5Y cells image acquisition was performed with a Leica confocal microscope SPE, and
526 Neuro-2a slides were analyzed using an Eclipse E600W Nikon microscope and images were

527 acquired with a Coolpix 5000 Nikon digital camera. γH2AX intensity measurements and
528 Rad51 foci number determinations were performed with CellProfiler cell image analysis
529 software.
530
531 *Slot-blot DNA repair assay*
532 SH-SY5Y cells were UV-irradiated and harvested at different time points post-irradiation.
533 Genomic DNA was isolated and equal amounts (200 ng) of DNA were spotted onto a nylon
534 membrane (Hybond N^+, GE Healthcare) with a slot-blot device (Life Technologies). DNA
535 was denatured by incubation of the membrane in 0.4 M NaOH for 20 minutes at room
536 temperature. The filter was further baked at 80°C for 2 h. UV-induced DNA lesions were
537 detected by immunoblot with 1:500 CPD antibody (Kamiya Biomedical, clone KTM53). The
538 membrane was also stained with Methylene Blue (Merck Millipore) for loading control,
539 according to the manufacturer's protocol.
540
541 *Caspase-3 activity assay*
542 SH-SY5Y cells were transfected with the specified ODN when indicated and exposed to
543 genotoxic agents. Cells were harvested 24 h later and incubated with lysis buffer (50 mM
544 Tris-HCl pH 7.4, 1 mM EDTA pH 8, 10 mM EGTA and 0.5 mM PMSF) at 37°C for 1 h with
545 vigorous vortexing every 15 min, and centrifuged at 10000 x *g* for 15 min. The activity of
546 caspase-3 in 150 µl cell lysate was determined using 150 µM of the synthetic caspase-3
547 substrate Ac-DEVD-pNA (Sigma-Aldrich) in reaction buffer (100 mM HEPES pH 7.5, 0.5
548 mM EDTA pH 8, 20% v/v glycerol and 5 mM dithiothreitol) in a final volume of 300 µl and
549 incubated at 37°C for 10 h. Color development was measured at 405 nm and caspase-3
550 activity was estimated as A_{405}/µg protein h.
551

552 *MTT assay*

553 SH-SY5Y cells were transfected with the specified ODN as described above. After 18 h, UV
554 irradiation was carried out and cells were further incubated for the indicated times. Cell
555 activity was assessed by 3-[4,5-dimethylthiazol-2-yl]-2,5-diphenyltetrazolium bromide
556 (MTT, Sigma-Aldrich) assay as described previously.[63]

557

558 *Clonogenic assay*

559 SH-SY5Y cells plated as single cell in 24-well plates (aprox. 100 cells/well), were transfected
560 with the indicated ODN and 18 h later were treated with the specified genotoxics. After 10
561 days, colonies were stained as previously described.[64]

562

563 *Chromatin isolation*

564 Chromatin isolation was carried out as described, [65] with minor modifications. Briefly, $1x10^{7}$
565 SH-SY5Y cells were resuspended in 300 µl of buffer A (10 mM HEPES pH 7.9, 10 mM KCl,
566 1.5 mM $MgCl_2$, 0.34 M sucrose, 10% glycerol, 1 mM DTT and 1X protease inhibitor cocktail
567 (Calbiochem)), 0.1% Triton X-100 was added and the cells were incubated on ice for 5 min.
568 Nuclei were obtained in the pellet after low-speed centrifugation (4 min, 1300 x *g*, 4°C). The
569 supernatant was clarified following high-speed centrifugation (15 min, 16,000 x *g*, 4°C) to
570 collect the cytoplasmic soluble fraction. Nuclei were washed in buffer A, and lysed in 200 µl
571 of buffer B (3 mM EDTA, 0.2 mM EGTA, 1 mM DTT and 1X protease inhibitor cocktail
572 (Calbiochem)) 30 min on ice. Insoluble chromatin was obtained by centrifugation (5 min,
573 1700 x *g*, 4°C), washed in buffer B, centrifuged again and the final chromatin pellet was
574 resuspended in 200 µl of Laemmli buffer and sonicated twice for 15 sec in a Fisher Sonic
575 Dismembrator Model 300 sonicator at 50% power. Cytoplasmic and chromatin fractions were
576 analyzed by immunoblotting (see *Western blotting analysis*).

577

578 *Live-cell imaging and microirradiation*

579 SH-SY5Y cells were transfected with E2F1-GFP or E2F2-GFP plasmids. Live-cell imaging
580 was carried out as previously described, [34] with a Nikon A1 inverted confocal microscope
581 with an environmental chamber that allows the control of temperature, humidity and gas
582 conditions. Microirradiation was performed for ~6 sec in preselected regions of 1 μm^2, with a
583 405 nm diode laser at 10% power. Confocal image series of a mid *z*-section were acquired
584 every 1 s with the 488 nm laser at 5% power, during the 6 sec before irradiation and for 1 min
585 following irradiation. Fluorescence intensities of the microirradiated region were expressed
586 relative to the immediate post-irradiation intensity for the recruitment kinetics analysis. Five
587 minutes before irradiation, 5 μM Ro 19-8022 photosensitizer was added to the medium when
588 indicated.

589

590 *Chromatin Immunoprecipitation and Slot-blot*

591 SH-SY5Y cells were transfected with E2F1-HA, E2F2-HA or JNK-HA plasmids, UV-
592 irradiated or mock-treated and 30 min later in vivo cross-linking and chromatin
593 immunoprecipitation (ChIP) was performed as previously reported,[66] with some
594 modifications. In brief, cells were fixed with 1% formaldehyde for 10 min at room
595 temperature and further incubated for 5 min with 0.125 M glycine solution at room
596 temperature. Cells were lysed in RIPA buffer and sonicated twelve times for 15 sec in a
597 Fisher Sonic Dismembrator Model 300 sonicator at 50% power. ChIP was carried out at 4°C
598 overnight with 4 μl of HA antibody (Covance, clone 16B12) along with 20 μl of protein A/G
599 PLUS-agarose beads (sc-2003). The precipitated DNA was reverse cross-linked, purified and
600 quantified. UV-induced DNA lesions were detected as described for the *Slot-blot DNA repair*
601 *assay*.

602

603 *Co-immunoprecipitation*

604 Whole-cell lysates (1 mg of protein diluted to 1 ml RIPA buffer) from SH-SY5Y cells treated
605 with the DNA damaging agent and harvested at the indicated times were subjected to
606 immunoprecipitation at 4°C overnight with 1 µg of E2F1 (sc-251), E2F2 (sc-9967) or E2F4
607 (sc-866) antibodies, along with 20 µl of protein A/G PLUS-agarose beads (sc-2003). Isotype
608 IgG control antibody (sc-2025) served as control. The beads were washed three times in PBS,
609 20 µl of Laemmli buffer was added, and the samples were analyzed by immunoblotting (see
610 *Western blotting analysis*).

611

612 *Triton X-100 cell fractionation*

613 SH-SY5Y cells were transfected with the indicated ODN and 18 h later were exposed to UV
614 irradiation and harvested at the indicated times. Biochemical fractionation into Triton X-100
615 soluble and insoluble fractions was performed as previously described. [67] Equal amounts of
616 proteins from each fraction were analyzed by immunoblotting (see *Western blotting*
617 *analysis*).

618

619 *Data analysis*

620 Data analysis was performed with GraphPad Prizm 5.0 (GraphPad Software, La Jolla, CA,
621 USA). Statistical differences were assessed by analysis of variance (ANOVA) with Tukey
622 *post hoc* analysis for multiple comparisons or with Dunnett *post hoc* analysis for multiple
623 comparisons to one control group. Student's *t*-test was applied when only two independent
624 groups were compared. *P*-values of <0.05 were considered significant.

625

626 **ACKNOWLEDGEMENTS**

This study was supported by research grants from Agencia Nacional de Promoción Científica y Tecnológica [PICT622]; Universidad de Buenos Aires [UBACYT20020100100284]; and Fondation ARC [PJA20131200165] to JPR. Exchanges between the Argentinian and French laboratories were supported by the Ministerio de Ciencia, Tecnología e Innovación Productiva and the French Ministry of Foreign Affairs through an Ecos-Sud Project [A09B01]. We thank Thierry Kortulewski at the IRCM Microscopy Facility for his help with the use of the video confocal microscope.

CONFLICTS OF INTEREST

The authors declare that they have no conflict of interest.

REFERENCES

1. Leone G, Nuckolls F, Ishida S, Adams M, Sears R, Jakoi L, Miron A, Nevins JR. Identification of a novel E2F3 product suggests a mechanism for determining specificity of repression by Rb proteins. Mol Cell Biol 2000; 20:3626-32.
2. He Y, Armanious MK, Thomas MJ, Cress WD. Identification of E2F-3B, an alternative form of E2F-3 lacking a conserved N-terminal region. Oncogene 2000; 19:3422-33.
3. Cartwright P, Muller H, Wagener C, Holm K, Helin K. E2F-6: a novel member of the E2F family is an inhibitor of E2F-dependent transcription. Oncogene 1998; 17:611-23.
4. Gaubatz S, Wood JG, Livingston DM. Unusual proliferation arrest and transcriptional control properties of a newly discovered E2F family member, E2F-6. Proc Natl Acad Sci U S A 1998; 95:9190-5.

652 5. Di Stefano L, Jensen MR, Helin K. E2F7, a novel E2F featuring DP-independent
653 repression of a subset of E2F-regulated genes. EMBO J 2003; 22:6289-98.
654 6. Christensen J, Cloos P, Toftegaard U, Klinkenberg D, Bracken AP, Trinh E, Heeran M,
655 Di Stefano L, Helin K. Characterization of E2F8, a novel E2F-like cell-cycle regulated
656 repressor of E2F-activated transcription. Nucleic Acids Res 2005; 33:5458-70.
657 7. Bagchi S, Raychaudhuri P, Nevins JR. Adenovirus E1A proteins can dissociate
658 heteromeric complexes involving the E2F transcription factor: a novel mechanism for E1A
659 trans-activation. Cell 1990; 62:659-69.
660 8. Lavia P, Jansen-Durr P. E2F target genes and cell-cycle checkpoint control. Bioessays
661 1999; 21:221-30.
662 9. Huang Y, Ishiko T, Nakada S, Utsugisawa T, Kato T, Yuan ZM. Role for E2F in DNA
663 damage-induced entry of cells into S phase. Cancer Res 1997; 57:3640-3.
664 10. Blattner C, Sparks A, Lane D. Transcription factor E2F-1 is upregulated in response to
665 DNA damage in a manner analogous to that of p53. Mol Cell Biol 1999; 19:3704-13.
666 11. O'Connor DJ, Lu X. Stress signals induce transcriptionally inactive E2F-1 independently
667 of p53 and Rb. Oncogene 2000; 19:2369-76.
668 12. Lin WC, Lin FT, Nevins JR. Selective induction of E2F1 in response to DNA damage,
669 mediated by ATM-dependent phosphorylation. Genes Dev 2001; 15:1833-44.
670 13. Ma Y, Freeman SN, Cress WD. E2F4 deficiency promotes drug-induced apoptosis.
671 Cancer Biol Ther 2004; 3:1262-9.
672 14. Martinez LA, Goluszko E, Chen HZ, Leone G, Post S, Lozano G, Chen Z, Chauchereau
673 A. E2F3 is a mediator of DNA damage-induced apoptosis. Mol Cell Biol 2010; 30:524-36.
674 15. Zalmas LP, Zhao X, Graham AL, Fisher R, Reilly C, Coutts AS, La Thangue NB. DNA-
675 damage response control of E2F7 and E2F8. EMBO Rep 2008; 9:252-9.

676 16. Biswas AK, Johnson DG. Transcriptional and nontranscriptional functions of E2F1 in
677 response to DNA damage. Cancer Res 2012; 72:13-7.
678 17. Stevens C, Smith L, La Thangue NB. Chk2 activates E2F-1 in response to DNA damage.
679 Nat Cell Biol 2003; 5:401-9.
680 18. Ianari A, Gallo R, Palma M, Alesse E, Gulino A. Specific role for p300/CREB-binding
681 protein-associated factor activity in E2F1 stabilization in response to DNA damage. J Biol
682 Chem 2004; 279:30830-5.
683 19. Galbiati L, Mendoza-Maldonado R, Gutierrez MI, Giacca M. Regulation of E2F-1 after
684 DNA damage by p300-mediated acetylation and ubiquitination. Cell Cycle 2005; 4:930-9.
685 20. Ferreira R, Magnaghi-Jaulin L, Robin P, Harel-Bellan A, Trouche D. The three members
686 of the pocket proteins family share the ability to repress E2F activity through recruitment of a
687 histone deacetylase. Proc Natl Acad Sci U S A 1998; 95:10493-8.
688 21. Vandel L, Nicolas E, Vaute O, Ferreira R, Ait-Si-Ali S, Trouche D. Transcriptional
689 repression by the retinoblastoma protein through the recruitment of a histone
690 methyltransferase. Mol Cell Biol 2001; 21:6484-94.
691 22. Strober BE, Dunaief JL, Guha, Goff SP. Functional interactions between the
692 hBRM/hBRG1 transcriptional activators and the pRB family of proteins. Mol Cell Biol 1996;
693 16:1576-83.
694 23. Martinez-Balbas MA, Bauer UM, Nielsen SJ, Brehm A, Kouzarides T. Regulation of
695 E2F1 activity by acetylation. EMBO J 2000; 19:662-71.
696 24. Morris L, Allen KE, La Thangue NB. Regulation of E2F transcription by cyclin E-Cdk2
697 kinase mediated through p300/CBP co-activators. Nat Cell Biol 2000; 2:232-9.
698 25. Chen J, Zhu F, Weaks RL, Biswas AK, Guo R, Li Y, Johnson DG. E2F1 promotes the
699 recruitment of DNA repair factors to sites of DNA double-strand breaks. Cell Cycle 2011;
700 10:1287-94.

701 26. Guo R, Chen J, Zhu F, Biswas AK, Berton TR, Mitchell DL, Johnson DG. E2F1
702 localizes to sites of UV-induced DNA damage to enhance nucleotide excision repair. J Biol
703 Chem 2010; 285:19308-15.
704 27. Guo R, Chen J, Mitchell DL, Johnson DG. GCN5 and E2F1 stimulate nucleotide
705 excision repair by promoting H3K9 acetylation at sites of damage. Nucleic Acids Res 2011;
706 39:1390-7.
707 28. Carcagno AL, Ogara MF, Sonzogni SV, Marazita MC, Sirkin PF, Ceruti JM, Canepa ET.
708 E2F1 transcription is induced by genotoxic stress through ATM/ATR activation. IUBMB
709 Life 2009; 61:537-43.
710 29. Dogra SC, Hahn CN, May BK. Superinduction by cycloheximide of cytochrome
711 P4502H1 and 5-aminolevulinate synthase gene transcription in chick embryo liver. Arch
712 Biochem Biophys 1993; 300:531-4.
713 30. Hiebert SW, Chellappan SP, Horowitz JM, Nevins JR. The interaction of RB with E2F
714 coincides with an inhibition of the transcriptional activity of E2F. Genes Dev 1992; 6:177-85.
715 31. Park KK, Deok Ahn J, Lee IK, Magae J, Heintz NH, Kwak JY, Lee YC, Cho YS, Kim
716 HC, Chae YM, et al. Inhibitory effects of novel E2F decoy oligodeoxynucleotides on
717 mesangial cell proliferation by coexpression of E2F/DP. Biochem Biophys Res Commun
718 2003; 308:689-97.
719 32. Sharma A, Singh K, Almasan A. Histone H2AX phosphorylation: a marker for DNA
720 damage. Methods Mol Biol 2012; 920:613-26.
721 33. Will O, Gocke E, Eckert I, Schulz I, Pflaum M, Mahler HC, Epe B. Oxidative DNA
722 damage and mutations induced by a polar photosensitizer, Ro19-8022. Mutat Res 1999;
723 435:89-101.

724 34. Campalans A, Kortulewski T, Amouroux R, Menoni H, Vermeulen W, Radicella JP.
725 Distinct spatiotemporal patterns and PARP dependence of XRCC1 recruitment to single-
726 strand break and base excision repair. Nucleic Acids Res 2013; 41:3115-29.
727 35. Krejci L, Altmannova V, Spirek M, Zhao X. Homologous recombination and its
728 regulation. Nucleic Acids Res 2012; 40:5795-818.
729 36. Mladenov E, Anachkova B, Tsaneva I. Sub-nuclear localization of Rad51 in response to
730 DNA damage. Genes Cells 2006; 11:513-24.
731 37. Brand M, Moggs JG, Oulad-Abdelghani M, Lejeune F, Dilworth FJ, Stevenin J,
732 Almouzni G, Tora L. UV-damaged DNA-binding protein in the TFTC complex links DNA
733 damage recognition to nucleosome acetylation. EMBO J 2001; 20:3187-96.
734 38. Beckmann AM, Wilce PA. Egr transcription factors in the nervous system. Neurochem
735 Int 1997; 31:477-510; discussion 7-6.
736 39. Quinones A, Dobberstein KU, Rainov NG. The egr-1 gene is induced by DNA-damaging
737 agents and non-genotoxic drugs in both normal and neoplastic human cells. Life Sci 2003;
738 72:2975-92.
739 40. Shin SY, Kim CG, Lee YH. Egr-1 regulates the transcription of the BRCA1 gene by
740 etoposide. BMB Rep 2013; 46:92-6.
741 41. Hallahan DE, Dunphy E, Virudachalam S, Sukhatme VP, Kufe DW, Weichselbaum RR.
742 C-jun and Egr-1 participate in DNA synthesis and cell survival in response to ionizing
743 radiation exposure. J Biol Chem 1995; 270:30303-9.
744 42. Huang RP, Fan Y, deBelle I, Ni Z, Matheny W, Adamson ED. Egr-1 inhibits apoptosis
745 during the UV response: correlation of cell survival with Egr-1 phosphorylation. Cell Death
746 Differ 1998; 5:96-106.

747 43. Pediconi N, Ianari A, Costanzo A, Belloni L, Gallo R, Cimino L, Porcellini A, Screpanti
748 I, Balsano C, Alesse E, et al. Differential regulation of E2F1 apoptotic target genes in
749 response to DNA damage. Nat Cell Biol 2003; 5:552-8.
750 44. Yoshida K, Inoue I. Expression of MCM10 and TopBP1 is regulated by cell proliferation
751 and UV irradiation via the E2F transcription factor. Oncogene 2004; 23:6250-60.
752 45. Kowalik TF, DeGregori J, Leone G, Jakoi L, Nevins JR. E2F1-specific induction of
753 apoptosis and p53 accumulation, which is blocked by Mdm2. Cell Growth Differ 1998;
754 9:113-8.
755 46. Vigo E, Muller H, Prosperini E, Hateboer G, Cartwright P, Moroni MC, Helin K.
756 CDC25A phosphatase is a target of E2F and is required for efficient E2F-induced S phase.
757 Mol Cell Biol 1999; 19:6379-95.
758 47. Ziebold U, Reza T, Caron A, Lees JA. E2F3 contributes both to the inappropriate
759 proliferation and to the apoptosis arising in Rb mutant embryos. Genes Dev 2001; 15:386-91.
760 48. DeGregori J. E2F and cell survival: context really is key. Dev Cell 2005; 9:442-4.
761 49. Wikonkal NM, Remenyik E, Knezevic D, Zhang W, Liu M, Zhao H, Berton TR,
762 Johnson DG, Brash DE. Inactivating E2f1 reverts apoptosis resistance and cancer sensitivity
763 in Trp53-deficient mice. Nat Cell Biol 2003; 5:655-60.
764 50. Berton TR, Mitchell DL, Guo R, Johnson DG. Regulation of epidermal apoptosis and
765 DNA repair by E2F1 in response to ultraviolet B radiation. Oncogene 2005; 24:2449-60.
766 51. Liu K, Lin FT, Ruppert JM, Lin WC. Regulation of E2F1 by BRCT domain-containing
767 protein TopBP1. Mol Cell Biol 2003; 23:3287-304.
768 52. Maser RS, Mirzoeva OK, Wells J, Olivares H, Williams BR, Zinkel RA, Farnham PJ,
769 Petrini JH. Mre11 complex and DNA replication: linkage to E2F and sites of DNA synthesis.
770 Mol Cell Biol 2001; 21:6006-16.

771 53. Chen D, Yu Z, Zhu Z, Lopez CD. E2F1 regulates the base excision repair gene XRCC1
772 and promotes DNA repair. J Biol Chem 2008; 283:15381-9.
773 54. Field SJ, Tsai FY, Kuo F, Zubiaga AM, Kaelin WG, Jr., Livingston DM, Orkin SH,
774 Greenberg ME. E2F-1 functions in mice to promote apoptosis and suppress proliferation. Cell
775 1996; 85:549-61.
776 55. Yamasaki L, Jacks T, Bronson R, Goillot E, Harlow E, Dyson NJ. Tumor induction and
777 tissue atrophy in mice lacking E2F-1. Cell 1996; 85:537-48.
778 56. Zhu JW, Field SJ, Gore L, Thompson M, Yang H, Fujiwara Y, Cardiff RD, Greenberg
779 M, Orkin SH, DeGregori J. E2F1 and E2F2 determine thresholds for antigen-induced T-cell
780 proliferation and suppress tumorigenesis. Mol Cell Biol 2001; 21:8547-64.
781 57. McKinnon PJ. DNA repair deficiency and neurological disease. Nat Rev Neurosci 2009;
782 10:100-12.
783 58. Caceres A, Banker GA, Binder L. Immunocytochemical localization of tubulin and
784 microtubule-associated protein 2 during the development of hippocampal neurons in culture.
785 J Neurosci 1986; 6:714-22.
786 59. Harris KF, Christensen JB, Radany EH, Imperiale MJ. Novel mechanisms of E2F
787 induction by BK virus large-T antigen: requirement of both the pRb-binding and the J
788 domains. Mol Cell Biol 1998; 18:1746-56.
789 60. Campanero MR, Flemington EK. Regulation of E2F through ubiquitin-proteasome-
790 dependent degradation: stabilization by the pRB tumor suppressor protein. Proc Natl Acad
791 Sci U S A 1997; 94:2221-6.
792 61. Chomczynski P, Sacchi N. Single-step method of RNA isolation by acid guanidinium
793 thiocyanate-phenol-chloroform extraction. Anal Biochem 1987; 162:156-9.

794 62. Varone CL, Giono LE, Ochoa A, Zakin MM, Canepa ET. Transcriptional regulation of
795 5-aminolevulinate synthase by phenobarbital and cAMP-dependent protein kinase. Arch
796 Biochem Biophys 1999; 372:261-70.
797 63. Ceruti JM, Scassa ME, Flo JM, Varone CL, Canepa ET. Induction of p19INK4d in
798 response to ultraviolet light improves DNA repair and confers resistance to apoptosis in
799 neuroblastoma cells. Oncogene 2005; 24:4065-80.
800 64. Ceruti JM, Scassa ME, Marazita MC, Carcagno AC, Sirkin PF, Canepa ET.
801 Transcriptional upregulation of p19INK4d upon diverse genotoxic stress is critical for
802 optimal DNA damage response. Int J Biochem Cell Biol 2009; 41:1344-53.
803 65. Mendez J, Stillman B. Chromatin association of human origin recognition complex,
804 cdc6, and minichromosome maintenance proteins during the cell cycle: assembly of
805 prereplication complexes in late mitosis. Mol Cell Biol 2000; 20:8602-12.
806 66. Fousteri M, Vermeulen W, van Zeeland AA, Mullenders LH. Cockayne syndrome A and
807 B proteins differentially regulate recruitment of chromatin remodeling and repair factors to
808 stalled RNA polymerase II in vivo. Mol Cell 2006; 23:471-82.
809 67. Gospodinov A, Tsaneva I, Anachkova B. RAD51 foci formation in response to DNA
810 damage is modulated by TIP49. Int J Biochem Cell Biol 2009; 41:925-33.
811
812 **FIGURE LEGENDS**
813
814 **FIGURE 1. *E2F1* and *E2F2* mRNA and protein levels increase following DNA damage**
815 **in neuronal cells. (A-B)** Northern blot analysis of SH-SY5Y cells treated with NCS, H_2O_2 or
816 UV and harvested at the specified times. Total RNA was extracted from cells and subjected
817 to Northern blot with the [^{32}P]-labelled probes shown in the left margin. In **(B)**, cells were
818 pre-incubated 3 h with 1 μM actinomycin D (Act D). The numbers under the bands indicate

819 *E2F1-5* quantitation normalized to β-tubulin and control in **(A)**, and *E2F1* and *E2F2*
820 quantitation normalized to β-tubulin and None (-) condition in **(B)**. **(C)** Western blot of E2F1
821 and E2F2 in SH-SY5Y cells treated with NCS, H_2O_2 or UV and harvested at the indicated
822 times. The numbers under the bands indicate E2F1 and E2F2 quantitation normalized to β-
823 actin and control. **(D-F)** Immunoblot of GFP in SH-SY5Y cells expressing E2F1-GFP **(D)**,
824 E2F2-GFP **(E)** or pEGFP-C1 empty vector **(F)** and harvested at the indicated times post-UV.
825 **(G-H)** Western blot of E2F1 and E2F2 in SH-SY5Y cells pre-incubated 3 h with 10 μM
826 cycloheximide (CHX) and harvested at the specified times after genotoxic treatment, as
827 shown in **(G)**. In **(D,E,F,H)**, data represent the mean±S.E.M. of at least four independent
828 experiments for **(D,E)** and n=3 for **(F,H)**. In **(D-F)**, *P*-values were calculated by one-way
829 ANOVA, Dunnett's: **P*<0.05, ***P*<0.01, n.s. not significant. C, control mock-treated cells.
830
831 **FIGURE 2. DNA damage induced E2F1 and E2F2 are transcriptionally active. (A)** CAT
832 activity of Neuro-2a cells transfected with pE2F-CAT or pΔE2F-CAT along with pCEFL-β-
833 galactosidase, and harvested 24 h post-genotoxic treatment. **(B-C)** CAT activity of Neuro-2a
834 cells transfected with pE2F-CAT, pCEFL-β-galactosidase and 1 μM of the indicated ODN,
835 and harvested 24 h after DNA damage. In all cases, CAT activity was normalized to β-
836 galactosidase activity. In **(B,C)**, results are expressed relative to None-ASLUC or None-mut
837 E2F DO conditions. Data represent the mean±S.E.M. of three independent experiments
838 performed in triplicate. *P*-values were obtained using one-way ANOVA with Tukey's
839 posttest in **(A)**, one-way ANOVA with Dunnett's posttest in **(B)** and Student's *t*-test in **(C)**:
840 **P*<0.05, ***P*<0.01, ****P*<0.001, n.s. not significant. DO, decoy oligodeoxynucleotide.
841
842 **FIGURE 3. *E2F1* and *E2F2* transcriptional upregulation requires ATM/ATR and MEK**
843 **kinases activity.** SH-SY5Y cells incubated 1 h with 5 mM caffeine, 10 μM KU-55933, 10

844 μM PD-98059, 50 μM LY-294002 or 25 μM SP-600125 and harvested after a 4 h treatment
845 with NCS, H_2O_2 or UV. Total RNA was extracted and subjected to Northern blot analysis
846 with the [^{32}P]-labelled probes shown in the left margin. The numbers under the bands indicate
847 *E2F1* and *E2F2* quantitation normalized to β-tubulin and None (-) condition.
848
849 **FIGURE 4. E2F1 and E2F2 upregulation reduces γH2AX intensity fo llowing UV**
850 **irradiation. (A)** SH-SY5Y cells expressing E2F1-GFP, E2F2-GFP or pEGFP-C1 empty
851 vector, fixed 30 minutes post-UV and immunostained with anti-γH2AX antibody. Nuclei
852 were visualized with DAPI staining. Scale bar, 10 μm. **(B-C)** Percentage of damaged cells
853 obtained by measurement of γH2AX intensity levels. Quantifications were carried out
854 classifying cells according to the E2F expression level: *no E2F*, *low E2F* or *high E2F* in **(B)**,
855 or to the GFP expression level: *no GFP*, *low GFP* or *high GFP* in **(C)**. Results are expressed
856 relative to mock-treated *no E2F* condition in **(B)** or mock-treated *no GFP* condition in **(C)**,
857 which represent the 10% of the maximum γH2AX intensity detected, and UV treatment was
858 normalized to mock-treatment for each of the E2F **(B)** or GFP **(C)** intensity levels. Data
859 represent the mean±S.E.M. of at least four independent experiments, in which 250 to 400
860 cells were analyzed for each condition. *P*-values were calculated by one-way ANOVA,
861 Tukey's: $^{**}P<0.01$, $^{***}P<0.001$, n.s. not significant. **(D)** Immunoblot of E2F1 or E2F2 in
862 SH-SY5Y cells transfected with E2F1-GFP or E2F2-GFP respectively, and in control not
863 transfected (NT) cells. Cells were harvested at the indicated times post-UV. E2F bands
864 correspond to the endogenous protein in NT and to the exogenously expressed protein in
865 E2F-GFP. The numbers under the bands indicate E2F1 and E2F2 quantitation normalized to
866 β-actin and NT-None condition.
867

868 **FIGURE 5. Blockade of E2F1 and E2F2 induction increases γH2AX intensity and**
869 **reduces DNA repair capability in response to DNA damage. (A-E)** Neuro-2A cells
870 transfected with 1 μM of the indicated ODN, exposed to NCS, H_2O_2 or UV **(A)** for 4 h **(B,D)**
871 or 10 h **(C,E)**, fixed and immunostained using anti-γH2AX antibody. Nuclei were visualized
872 with DAPI staining. Scale bar, 10 μm. In **(B-E)**, data represent the mean±S.E.M. of at least
873 three independent experiments, in which 300 to 1000 cells were analyzed for each condition.
874 The percentage of damaged cells was obtained by measurement of γH2AX intensity levels.
875 Quantifications were carried out so that data is expressed relative to the control ODNs
876 ASCAT or mut E2F DO, which represent the 10% of the maximum γH2AX intensity
877 detected. *P*-values were obtained by one-way ANOVA followed by Dunnett's posttest in
878 **(B,C)** and Student's *t*-test in **(D,E)**: *$P<0.05$, **$P<0.01$, ***$P<0.001$, n.s. not significant. **(F)**
879 SH-SY5Y cells transfected with 1 μM of the indicated ODN, UV-irradiated and harvested
880 immediately (0 h) or at 6, 24 or 48 h post-irradiation. Genomic DNA was slot-blotted and
881 analyzed by immunoblot for CPD photoproducts. Methylene Blue staining for total DNA was
882 used as a loading control. The table indicates the average of two independent experiments of
883 the percentage of remaining CPD photoproducts, obtained by CPD quantitation and
884 normalization to total DNA. DO, decoy oligodeoxynucleotide.
885
886 **FIGURE 6. E2F1 and E2F2 reduce apoptotic response after genotoxic stress.** SH-SY5Y
887 cells transfected with 1 μM of the specified ODN and treated with H_2O_2. **(A-B)** Cell lysates
888 examined for caspase-3 activity 24 h post-H_2O_2. **(C)** Western blot of anti-cleaved caspase-3 8
889 h post-H_2O_2. The numbers under the bands indicate cleaved caspase-3 quantitation
890 normalized to β-actin and control ODN. In **(A,B)**, data represent the mean±S.E.M. of four
891 independent experiments performed in duplicate. One-way ANOVA, Tukey's: *$P<0.05$,
892 **$P<0.01$, ***$P<0.001$, n.s. not significant. DO, decoy oligodeoxynucleotide.

893

894 **FIGURE 7. E2F1 and E2F2 confer cellular resistance to genotoxic stimuli. (A-B)** Cell
895 survival assessed by MTT reduction assay in SH-SY5Y cells transfected with 1 μM of the
896 specified ODN and exposed to UV irradiation. Data is representative of four independent
897 experiments carried out in octuplicate. **(C-E)** Clonogenic assay in SH-SY5Y cells transfected
898 with 1 μM of the indicated ODN and treated with the DNA damaging agent. In **(D,E)**, results
899 are expressed relative to the control mock-treated cells for each ODN, and data represent the
900 mean±S.E.M. of four independent experiments performed in cuadruplicate. *P*-values were
901 calculated using one-way ANOVA with Dunnett's posttest in **(D)** and Student's *t*-test in **(E)**:
902 **P*<0.05, ***P*<0.01, ****P*<0.001, n.s. not significant. DO, decoy oligodeoxynucleotide.

903

904 **FIGURE 8. Accumulation of E2F1 and E2F2 at sites of DNA damage. (A)** E2F1 and
905 E2F2 Western blot of cytoplasmic and chromatin fractions of SH-SY5Y cells treated with
906 genotoxic agents for the indicated times. GAPDH and H3 were used as cytoplasmic and
907 chromatin specific markers respectively. Data represents the cytoplasm and chromatin-
908 associated E2F relative percentages for each condition, obtained by normalization to GAPDH
909 and H3 correspondingly. **(B-E)** Live-cell imaging of SH-SY5Y cells expressing E2F1-GFP or
910 E2F2-GFP microirradiated with a 405 nm laser and pre-incubated or not with the
911 photosensitizer Ro 19-8022 (Ro). In **(C,E)**, data represent the mean±S.D. of two independent
912 experiments, in which 10 cells were analyzed for each condition. Arrows indicate the site of
913 microirradiation. Scale bar, 2 μm. **(F)** SH-SY5Y cells expressing E2F1-HA or E2F2-HA
914 (upper panel) or JNK-HA (lower panel) were UV-irradiated or mock-treated, fixed, lysed and
915 ChIP was carried out with anti-HA antibody. Pulled-down DNA was slot-blotted and
916 analyzed by immunoblot for CPD photoproducts. Methylene Blue staining for total DNA was
917 used as a loading control. **(G)** Co-immunoprecipitation assays of whole-cell lysates from SH-

918 SY5Y cells harvested 1 h post-NCS treatment. Immunoprecipitation (IP) was performed with
919 anti-E2F1, anti-E2F2 and anti-E2F4 antibodies and associated proteins were detected by
920 immunoblot (IB). Non specific IgG isotype antibody served as IP control.
921
922 **FIGURE 9. E2F2 promotes Rad51 foci formation and induces histone acetylation in**
923 **response to DNA damage. (A-B)** SH-SY5Y cells transfected with 1 μM of ASE2F2, fixed 1
924 h post-NCS treatment and immunostained using anti-Rad51 and anti-γH2AX antibodies.
925 Nuclei were visualized with DAPI staining. Scale bar, 10 μm. In **(B)** data represent the
926 mean±S.E.M. of four independent experiments, in which 100 to 250 cells were analyzed for
927 each condition. *P*-values were calculated using one-way ANOVA with Tukey's posttest:
928 **P*<0.05, ****P*<0.001, n.s. not significant. Cells with five or more Rad51 foci were
929 considered as positive Rad51 cells. **(C)** Rad51 immunoblot of Triton soluble (TS) and
930 insoluble (TI) fractions of SH-SY5Y cells transfected with 1 μM of ASE2F2 and harvested 1
931 h post-NCS treatment. GAPDH and H3 were used to detect soluble cytoplasmic and
932 chromatin-bound proteins respectively. The numbers under the bands indicate Rad51
933 quantitation normalized to GAPDH or H3 in TS or TI fractions correspondingly, and ASCAT
934 condition for each fraction. **(D)** Co-immunoprecipitation assay of whole-cell lysates from
935 SH-SY5Y cell harvested 30 minutes post-UV irradiation. Immunoprecipitation (IP) was
936 performed with anti-E2F2 antibody and associated proteins were detected by immunoblot
937 (IB). Non specific IgG isotype antibody served as IP control. **(E)** Western blot of acetylated
938 H4 (H4Ac) in SH-SY5Y cells transfected with 1 μM of ASE2F2 and harvested 2 or 30
939 minutes following UV light exposure. The numbers under the bands indicate H4Ac
940 quantitation normalized to H3 and ASCAT-control condition. C, control mock-treated cells.

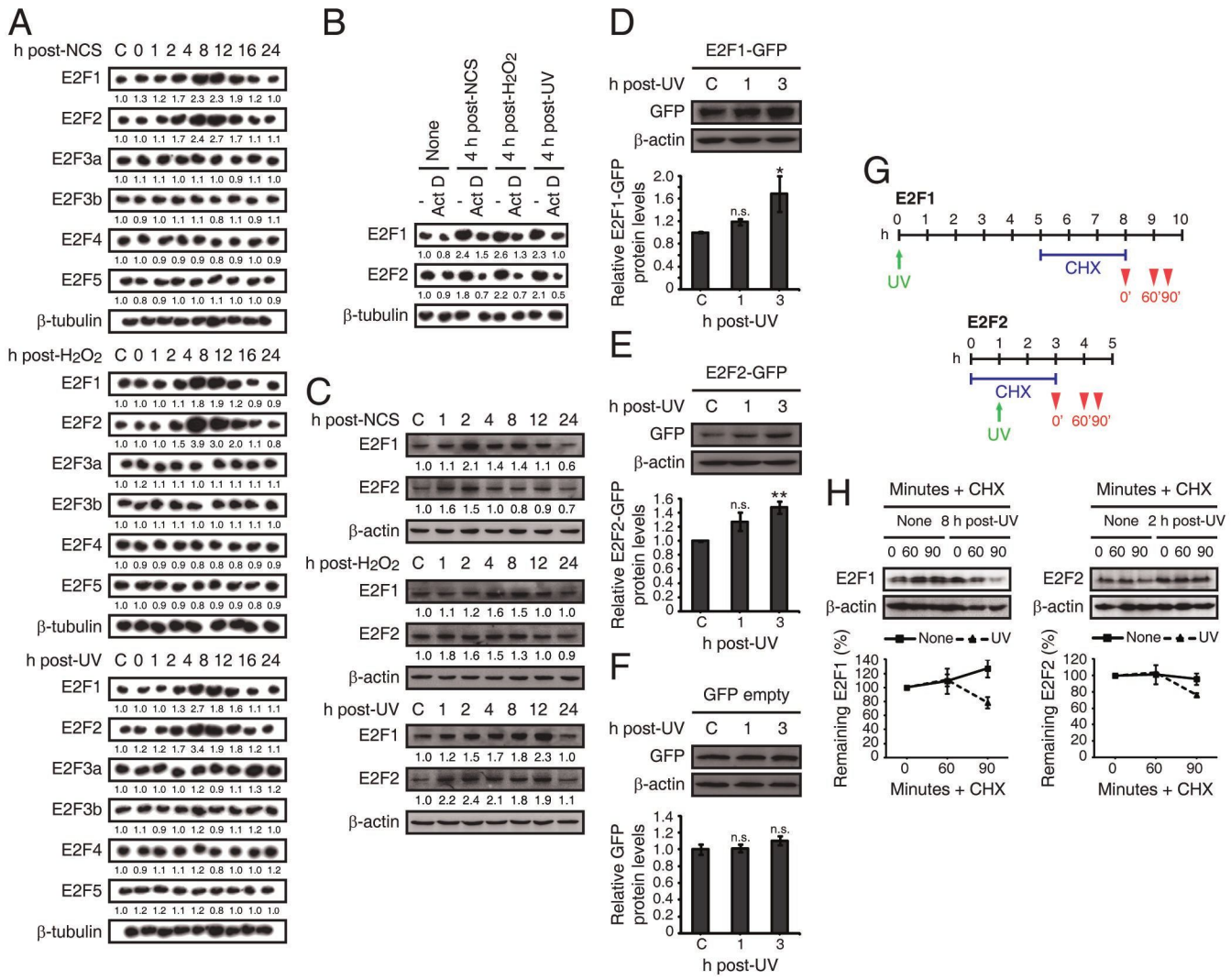
A
h post-NCS C 0 1 2 4 8 12 16 24
E2F1
1.0 1.3 1.2 1.7 2.3 2.3 1.9 1.2 1.0
E2F2
1.0 1.0 1.1 1.7 2.4 2.7 1.7 1.1 1.1
E2F3a
1.0 1.1 1.1 1.0 1.1 1.0 0.9 1.1 1.0
E2F3b
1.0 0.9 1.0 1.1 1.1 0.8 1.1 0.9 1.1
E2F4
1.0 1.0 0.9 0.9 0.9 0.8 0.9 1.0 0.9
E2F5
1.0 0.8 0.9 1.0 1.0 1.1 1.0 1.0 0.9
β-tubulin
h post-H2O2 C 0 1 2 4 8 12 16 24
E2F1
1.0 1.0 1.0 1.1 1.8 1.9 1.2 0.9 0.9
E2F2
1.0 1.0 1.0 1.5 3.9 3.0 2.0 1.1 0.8
E2F3a
1.0 1.2 1.1 1.1 1.0 1.1 1.1 1.1 1.1
E2F3b
1.0 1.0 1.1 1.1 1.0 1.0 1.1 1.1 1.0
E2F4
1.0 0.9 0.9 0.9 0.8 0.8 0.8 0.9 0.9
E2F5
1.0 1.0 0.9 0.9 0.8 0.9 0.9 0.8 0.9
β-tubulin
h post-UV C 0 1 2 4 8 12 16 24
E2F1
1.0 1.0 1.0 1.3 2.7 1.8 1.6 1.1 1.1
E2F2
1.0 1.2 1.2 1.7 3.4 1.9 1.8 1.2 1.1
E2F3a
1.0 1.0 1.0 1.0 1.2 0.9 1.1 1.3 1.2
E2F3b
1.0 1.1 0.9 1.0 1.2 0.9 1.1 1.2 1.0
E2F4
1.0 0.9 1.1 1.1 1.2 0.8 1.0 1.0 1.2
E2F5
1.0 1.2 1.2 1.1 1.2 0.8 1.0 1.0 1.0
β-tubulin
B
None
4 h post-NCS
4 h post-H2O2
4 h post-UV
- Act D - Act D - Act D - Act D
E2F1
1.0 0.8 2.4 1.5 2.6 1.3 2.3 1.0
E2F2
1.0 0.9 1.8 0.7 2.2 0.7 2.1 0.5
β-tubulin
C
h post-NCS C 1 2 4 8 12 24
E2F1
1.0 1.1 2.1 1.4 1.4 1.1 0.6
E2F2
1.0 1.6 1.5 1.0 0.8 0.9 0.7
β-actin
h post-H2O2 C 1 2 4 8 12 24
E2F1
1.0 1.1 1.2 1.6 1.5 1.0 1.0
E2F2
1.0 1.8 1.6 1.5 1.3 1.0 0.9
β-actin
h post-UV C 1 2 4 8 12 24
E2F1
1.0 1.2 1.5 1.7 1.8 2.3 1.0
E2F2
1.0 2.2 2.4 2.1 1.8 1.9 1.1
β-actin
D
E2F1-GFP
h post-UV C 1 3
GFP
β-actin
Relative E2F1-GFP protein levels
n.s.
*
h post-UV
E
E2F2-GFP
h post-UV C 1 3
GFP
β-actin
Relative E2F2-GFP protein levels
n.s.
**
h post-UV
F
GFP empty
h post-UV C 1 3
GFP
β-actin
Relative GFP protein levels
n.s.
n.s.
h post-UV
G
E2F1
h 0 1 2 3 4 5 6 7 8 9 10
UV
CHX
0' 60'90'
E2F2
h 0 1 2 3 4 5
CHX
UV
0' 60'90'
H
Minutes + CHX
None 8 h post-UV
0 60 90 0 60 90
E2F1
β-actin
Minutes + CHX
None 2 h post-UV
0 60 90 0 60 90
E2F2
β-actin
None UV
Remaining E2F1 (%)
Minutes + CHX
None UV
Remaining E2F2 (%)
Minutes + CHX

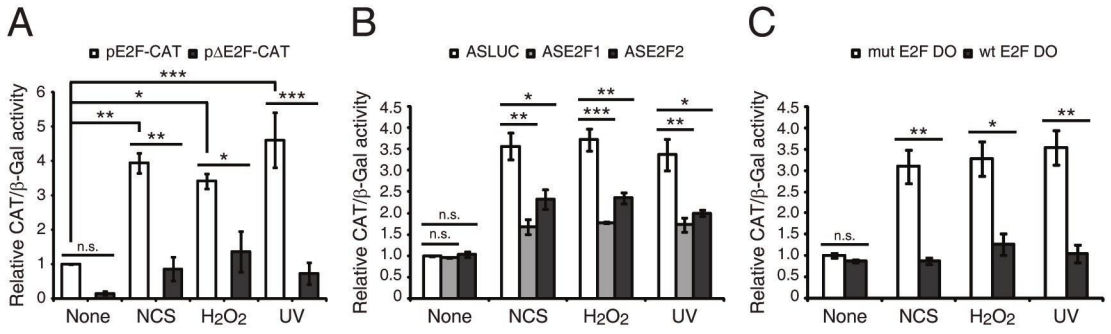
A
pE2F-CAT
pΔE2F-CAT
Relative CAT/β-Gal activity
0
1
2
3
4
5
6
n.s.
**
**
*
*
***
***
None
NCS
H2O2
UV
B
ASLUC
ASE2F1
ASE2F2
Relative CAT/β-Gal activity
0
0.5
1.0
1.5
2.0
2.5
3.0
3.5
4.0
4.5
n.s.
n.s.
*
**
**
***
*
**
None
NCS
H2O2
UV
C
mut E2F DO
wt E2F DO
Relative CAT/β-Gal activity
0
0.5
1.0
1.5
2.0
2.5
3.0
3.5
4.0
4.5
n.s.
**
*
**
None
NCS
H2O2
UV

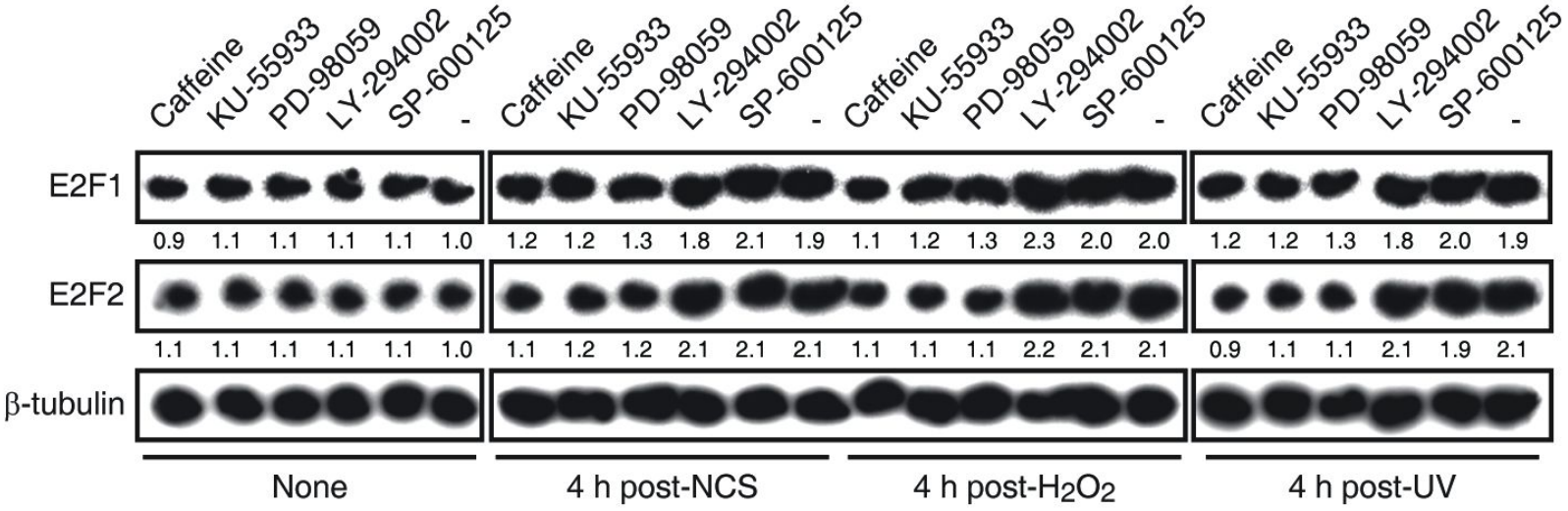
Caffeine
KU-55933
PD-98059
LY-294002
SP-600125
-
E2F1
0.9 1.1 1.1 1.1 1.1 1.0
1.2 1.2 1.3 1.8 2.1 1.9
1.1 1.2 1.3 2.3 2.0 2.0
1.2 1.2 1.3 1.8 2.0 1.9
E2F2
1.1 1.1 1.1 1.1 1.1 1.0
1.1 1.2 1.2 2.1 2.1 2.1
1.1 1.1 1.1 2.2 2.1 2.1
0.9 1.1 1.1 2.1 1.9 2.1
β-tubulin
None
4 h post-NCS
4 h post-H_2O_2
4 h post-UV

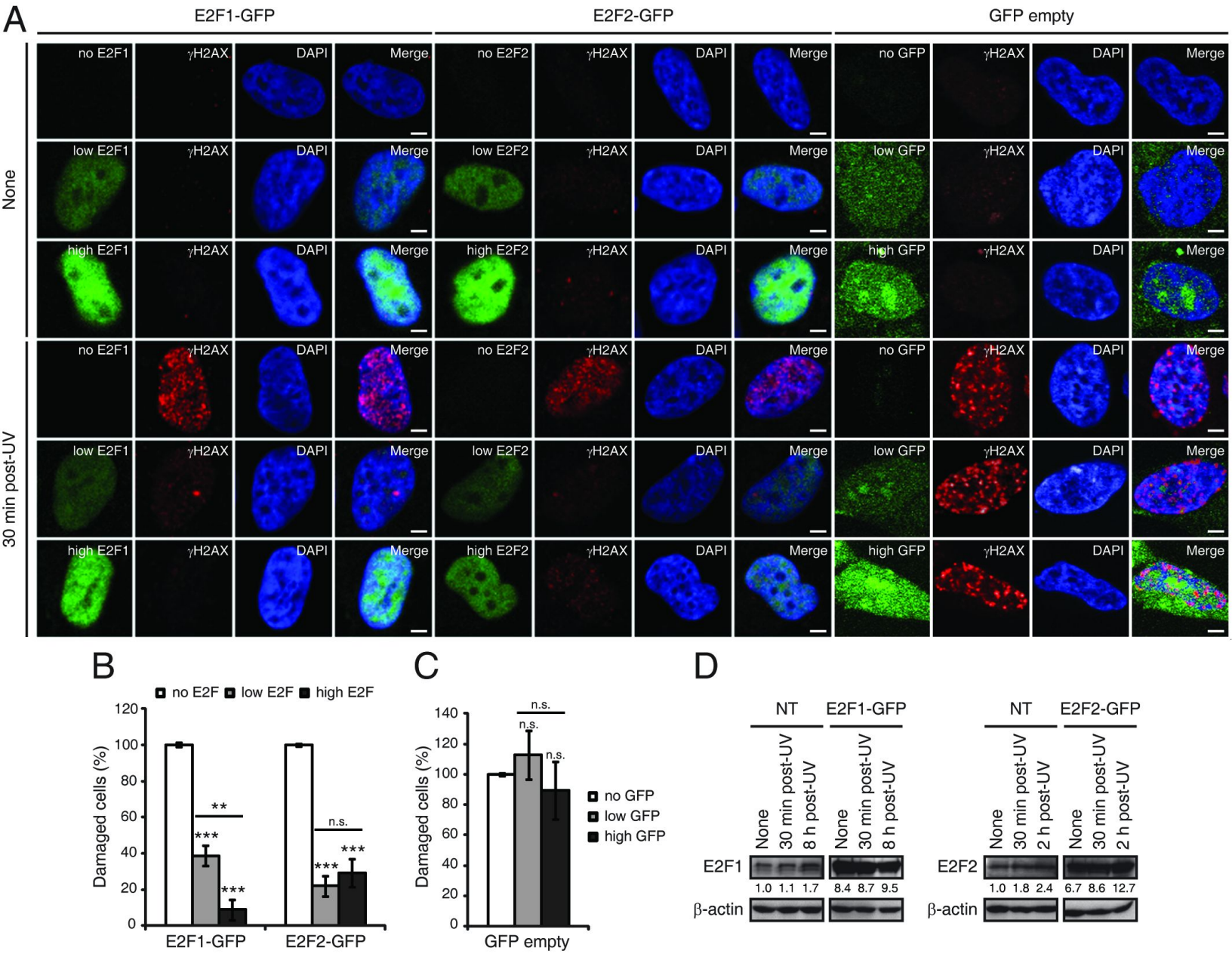
A
E2F1-GFP
E2F2-GFP
GFP empty
None
30 min post-UV
no E2F1
low E2F1
high E2F1
no E2F2
low E2F2
high E2F2
no GFP
low GFP
high GFP
γH2AX
DAPI
Merge
B
no E2F
low E2F
high E2F
Damaged cells (%)
120
100
80
60
40
20
0
**
***
n.s.
E2F1-GFP
E2F2-GFP
C
140
no GFP
low GFP
high GFP
GFP empty
D
NT
E2F1-GFP
E2F2-GFP
None
30 min post-UV
8 h post-UV
2 h post-UV
E2F1
E2F2
β-actin
1.0 1.1 1.7
8.4 8.7 9.5
1.0 1.8 2.4
6.7 8.6 12.7

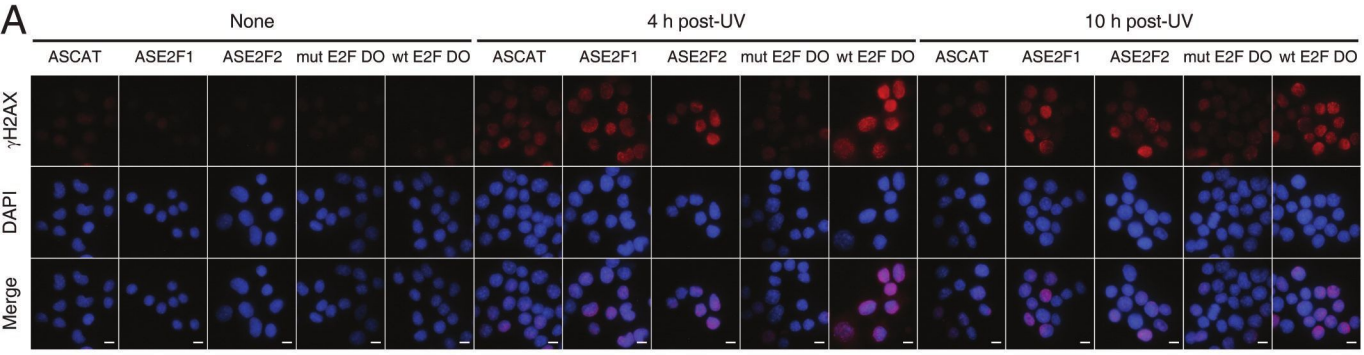

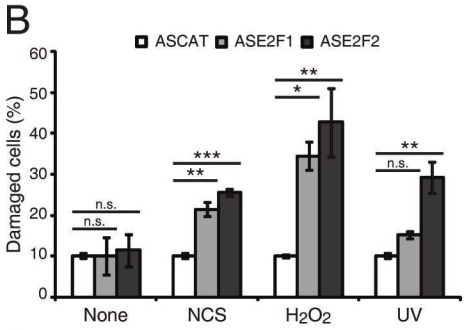

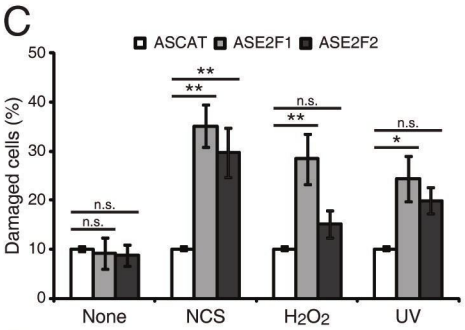

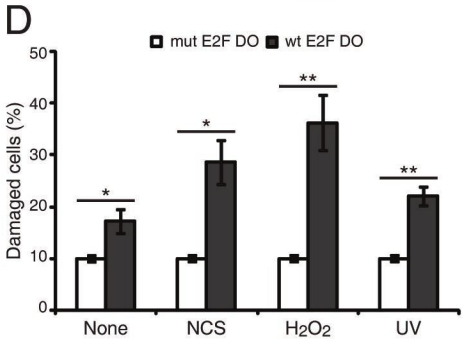

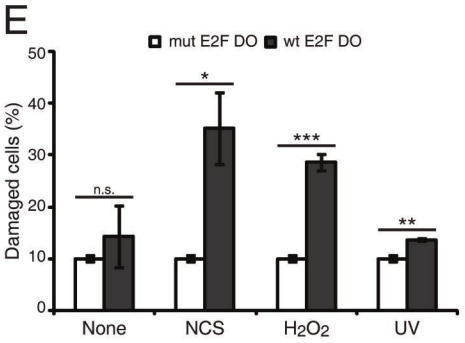

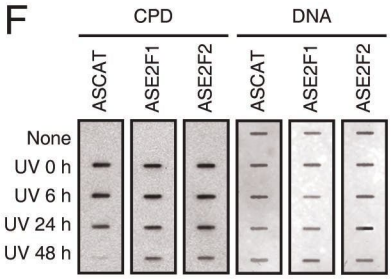

Remaining CPD (%)

	ASCAT	ASE2F1	ASE2F2
UV 0 h	100	100	100
UV 6 h	99	97	99
UV 24 h	76	94	95
UV 48 h	13	38	46

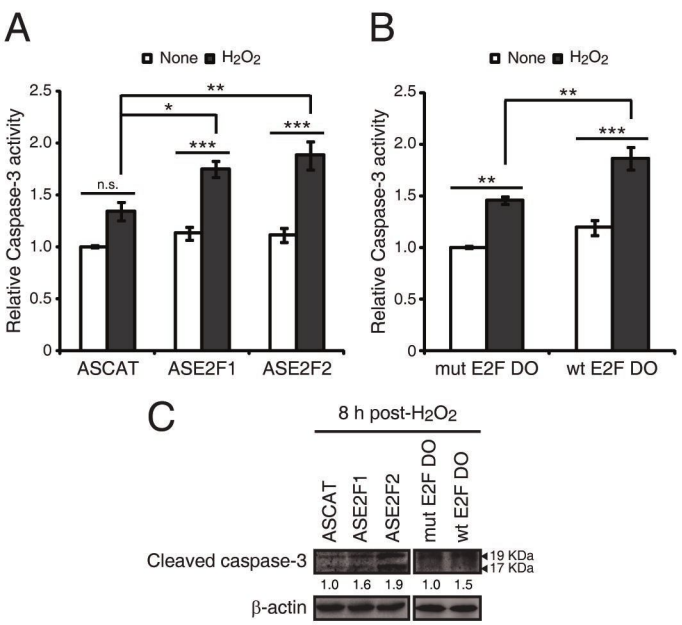
A
None
H_2O_2
Relative Caspase-3 activity
2.5
2.0
1.5
1.0
0.5
0
n.s.
*
**
***
***
ASCAT
ASE2F1
ASE2F2
B
None
H_2O_2
Relative Caspase-3 activity
**
**
***
mut E2F DO
wt E2F DO
C
8 h post-H_2O_2
ASCAT
ASE2F1
ASE2F2
mut E2F DO
wt E2F DO
Cleaved caspase-3
19 KDa
17 KDa
1.0
1.6
1.9
1.0
1.5
β-actin

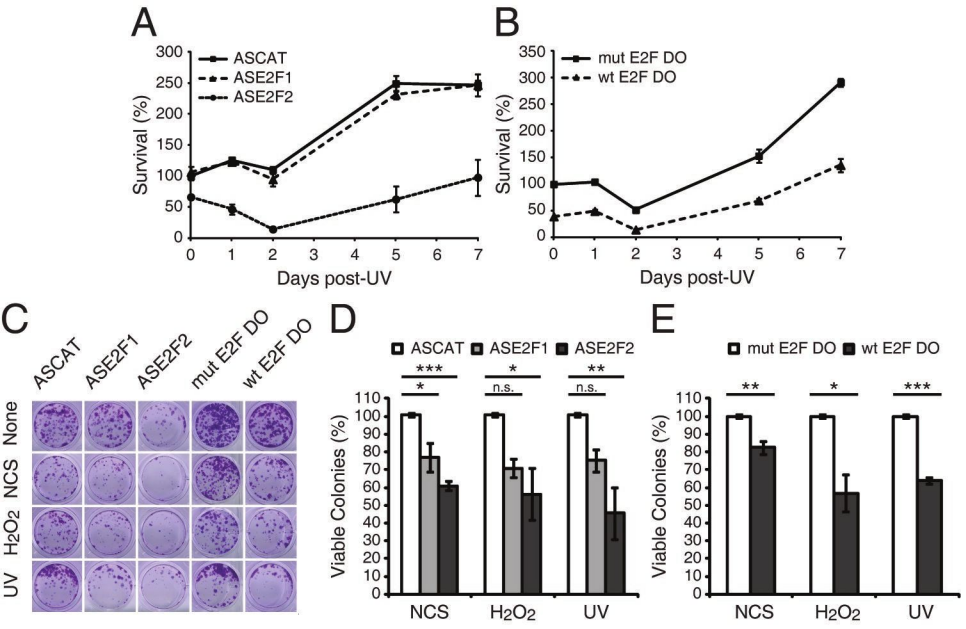
A
ASCAT
ASE2F1
ASE2F2
Survival (%)
Days post-UV
B
mut E2F DO
wt E2F DO
Survival (%)
Days post-UV
C
ASCAT
ASE2F1
ASE2F2
mut E2F DO
wt E2F DO
None
NCS
H2O2
UV
D
ASCAT
ASE2F1
ASE2F2
Viable Colonies (%)
NCS
H2O2
UV
n.s.
E
mut E2F DO
wt E2F DO
Viable Colonies (%)
NCS
H2O2
UV

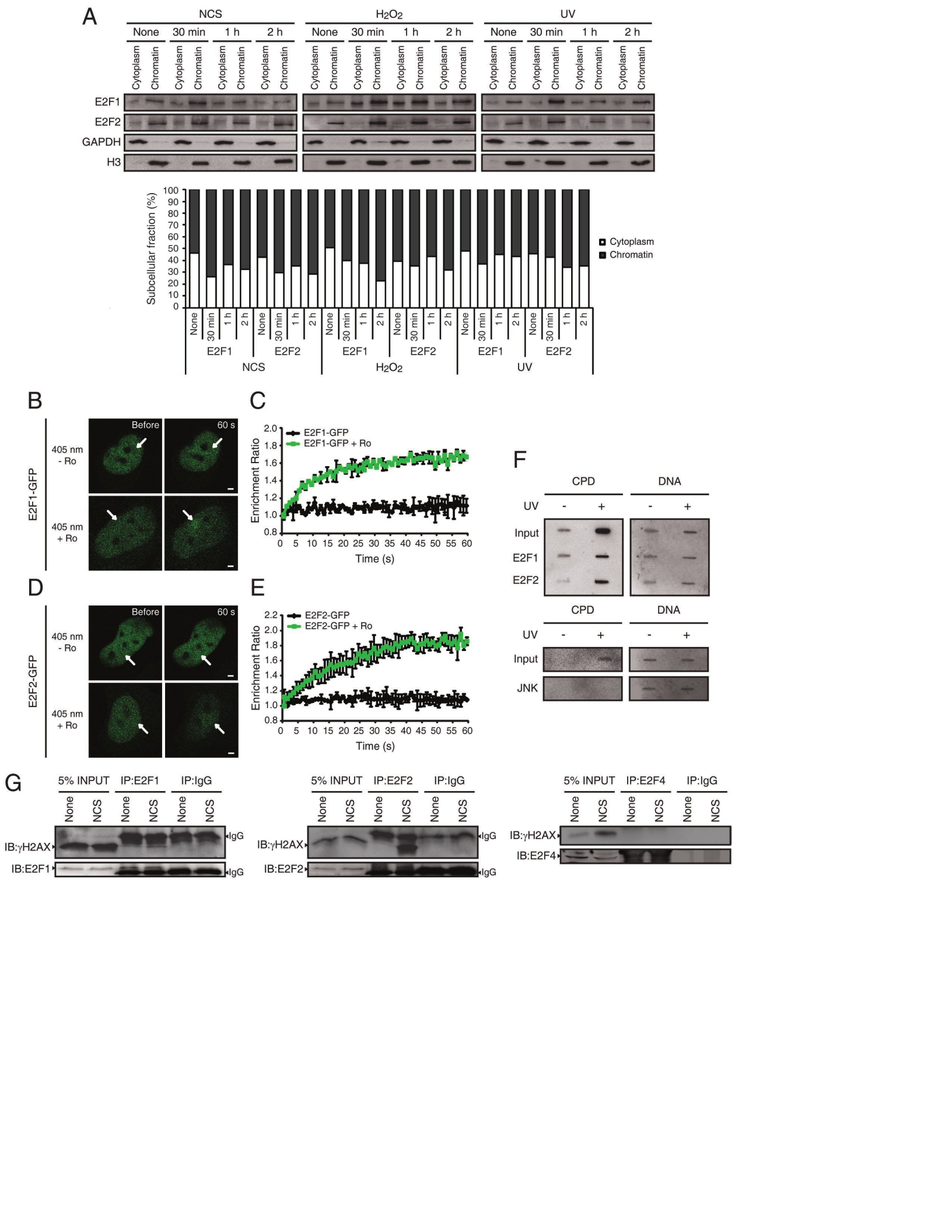
A
NCS
H2O2
UV
None
30 min
1 h
2 h
Cytoplasm
Chromatin
E2F1
E2F2
GAPDH
H3
Subcellular fraction (%)
Cytoplasm
Chromatin
B
E2F1-GFP
405 nm - Ro
405 nm + Ro
Before
60 s
C
E2F1-GFP
E2F1-GFP + Ro
Enrichment Ratio
Time (s)
D
E2F2-GFP
E
E2F2-GFP
E2F2-GFP + Ro
F
CPD
DNA
UV
Input
E2F1
E2F2
JNK
G
5% INPUT
IP:E2F1
IP:IgG
IP:E2F2
IP:E2F4
IB:γH2AX
IB:E2F1
IB:E2F2
IB:E2F4
IgG

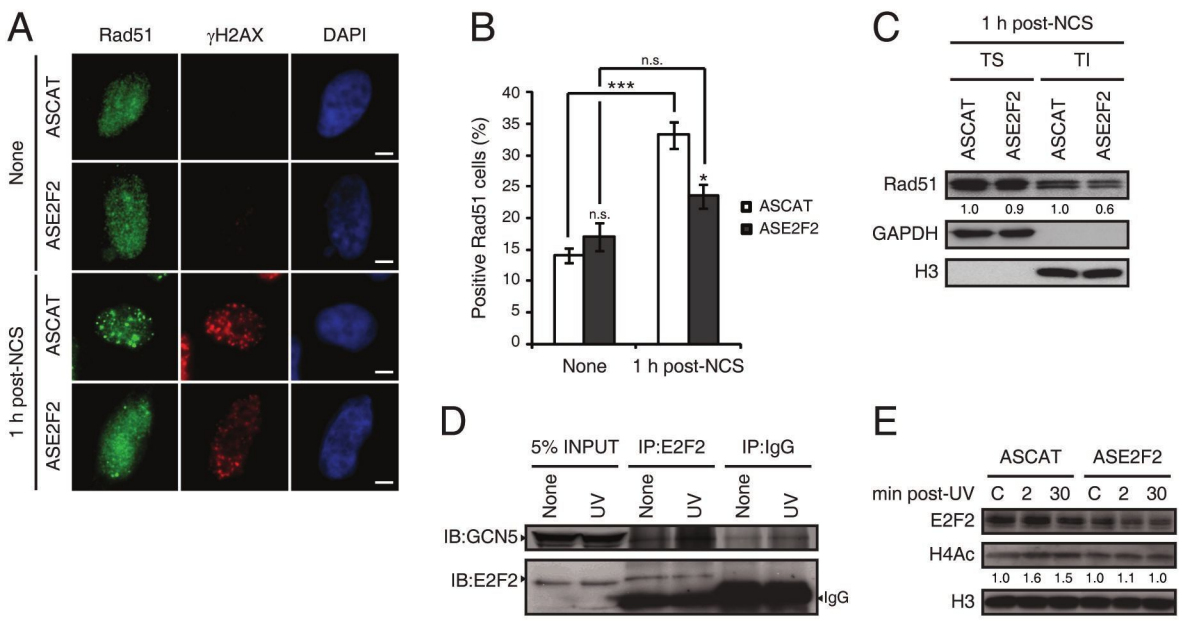
A
Rad51
γH2AX
DAPI
None
ASCAT
ASE2F2
1 h post-NCS
ASCAT
ASE2F2
B
n.s.
***
n.s.
*
Positive Rad51 cells (%)
40
35
30
25
20
15
10
5
0
None
1 h post-NCS
ASCAT
ASE2F2
C
1 h post-NCS
TS
TI
ASCAT
ASE2F2
ASCAT
ASE2F2
Rad51
1.0
0.9
1.0
0.6
GAPDH
H3
D
5% INPUT
IP:E2F2
IP:IgG
None
UV
None
UV
None
UV
IB:GCN5
IB:E2F2
IgG
E
ASCAT
ASE2F2
min post-UV
C
2
30
C
2
30
E2F2
H4Ac
1.0
1.6
1.5
1.0
1.1
1.0
H3